JOURNAL OF GEOPHYSICAL RESEARCH, VOL. 94, NO. B4, PAGES 4469–4496, APRIL 10, 1989

# Shoshonitic Volcanism in the Northern Mariana Arc 1. Mineralogic and Major and Trace Element Characteristics

SHERMAN H. BLOOMER[1]

*Department of Geology, Duke University, Durham, North Carolina*

ROBERT J. STERN

*Center for Lithospheric Studies, University of Texas at Dallas*

ELISHA FISK and C.H. GESCHWIND

*Department of Geology, Duke University, Durham, North Carolina*

Petrographic and geochemical characteristics of samples dredged from 23 submarine volcanic edifices in the northern Mariana and southern Volcano arcs define two distinct rock series. The central and northern Mariana Arc (to 23°N) and the northern Volcano Arc (north of Iwo Jima) are characterized by plagioclase-clinopyroxene-orthopyroxene-titantomagnetite bearing subalkaline rocks, including both low-K and medium-K series. The northern Mariana Arc and southern Volcano Arc, from 23°N to Iwo Jima, are erupting rocks of a shoshonitic series with phenocrysts of plagioclase, clinopyroxene, olivine, and biotite. These rocks are less saturated than those of the subalkaline provinces and are substantially enriched in Ba (400-900 ppm), Sr (600-1000 ppm), $K_2O$ (1-4.5%), and $K_2O/Na_2O$ (0.4-1.2) relative to the subalkaline lavas. Ba/Y and Ba/Zr increase by a factor of 3 to 4 in the shoshonitic rocks, but K/Rb, Ba/Sr, and K/Ba are relatively constant throughout the arc. There is no relationship between degree of enrichment and volcano volume or degree of fractionation: seamounts and islands within each province have the same range of compositions. Much of the intra-edifice variation in lava composition can be modeled by 10-70% crystallization of plagioclase and clinopyroxene, with smaller amounts of olivine, orthopyroxene, and titanomagnetite, or by accumulation of 10-40% phenocrysts, dominantly plagioclase. The differences between parental lavas in the alkalic and subalkalic provinces require melting of two distinct mantle sources. The occurrence of this enriched mantle in the northern Marianas may be a consequence of the propagation of the Mariana Trough spreading center into the Volcano Arc.

## Introduction

Intraoceanic island arcs provide the simplest setting in which to examine the characteristics and causes of volcanism associated with subduction. Most studies of intraoceanic arcs have concentrated on subaerial edifices because of their size and accessibility. The subaerial volcanic rocks, however, make up only a small part of the volume of material erupted in these arcs; over 90% of the material in arcs such as the Marianas or Tonga is erupted in a submarine setting. Over half the length of the presently active Mariana Arc is represented only by submarine volcanos [*Stern et al.*, 1988*b*]. If we are to develop a complete understanding of intraoceanic arc volcanism, it is essential that we have a detailed knowledge of the volcanological and geochemical characteristics of the submarine portions of intraoceanic arcs.

A number of models have been proposed for spatial and temporal variability in the petrochemistry of intraoceanic arcs. These include models for a temporal evolution of arc volcanism through tholeiitic, calcalkalic and shoshonitic stages at a given distance from the trench, and for a spatial distribution of volcanism from tholeiitic to calcalkalic to shoshonitic with increasing distance from a trench [*Jakes and Gill*, 1970; *Jakes and White* 1972; *Barberi et al.*, 1974; *Lefevre*, 1973; *Whitford and Nicholls*, 1976; *Gill*, 1981]. One complication for simple models of arc evolution in intraoceanic arcs is the development of back arc basins and the consequent reestablishment of the arc after such rifting. We do not know what the chemical effects of this cyclicity in arc volcanism are. The arc, after back arc rifting, could simply continue to erupt the same compositions as it did prior to the rifting or it could return to an earlier phase of its chemical evolution. Detailed studies of the submarine portions of active, intraoceanic arcs are essential for evaluation of models for temporal and spatial arc evolution.

We present here the preliminary results of part of a detailed study of submarine volcanos in the northern Mariana and southern Volcano arcs. We discuss the petrographic, major element, and trace element characteristics of the lavas from these volcanos; the large-ion-incompatible and rare earth element (REE) concentrations of the same lavas are presented in a companion paper [*Lin et al.*, this issue]. The data show that the arc comprises a subalkalic province and an alkalic province with shoshonitic affinities. The alkalic province is characterized by high K/Na, and high abundances of alkali and alkaline-earth elements. The influences of crystal fractionation and accumulation, partial melting variations, and source heterogeneity on the origins of these rocks are explored, and some of the implications of these data for models of arc evolution are discussed.

[1]Now at Department of Geology, Boston University, Massachusetts



Paper number 88JB03734.
0148-0227/89/88JB-3734$05.00

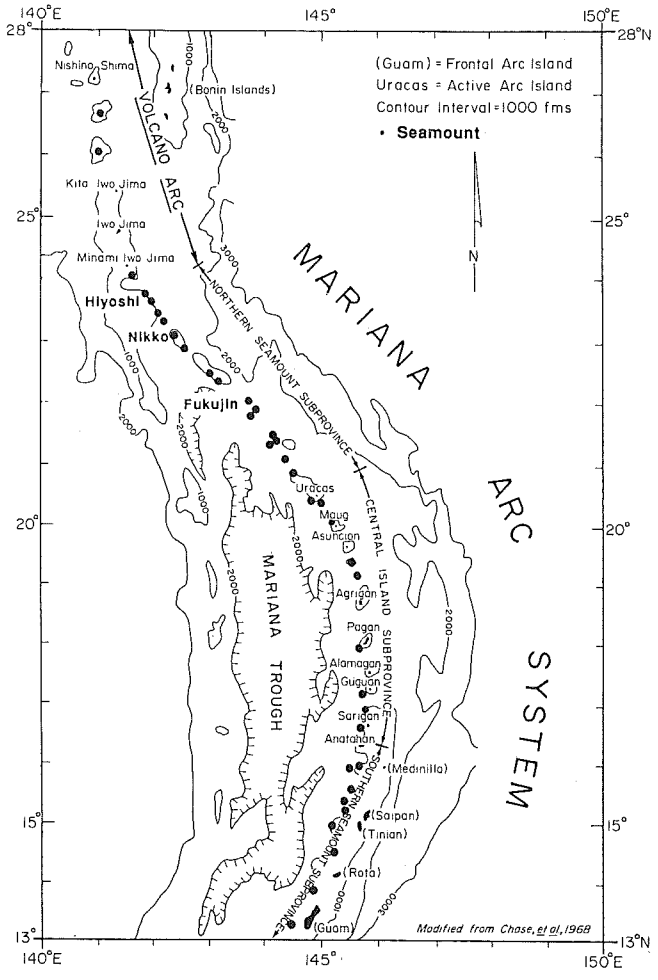


Fig. 1. Location of major volcanic provinces in the Mariana Arc after *Dixon and Stern* [1983] and *Stern et al.* [1988a]. Large dots indicate positions of submarine volcanos. Detailed bathymetric charts of the volcanos discussed here are included in *Lin et al.* (this volume).

## BACKGROUND

The Volcano and Mariana arcs are part of the 2400-km magmatic arc associated with the subduction of the Pacific plate beneath the Philippine Sea plate. The Volcano Arc extends from 27°N to 24°N and includes both subaerial and submarine edifices which form the Shichito Ridge [*Honza and Tamaki*, 1985]. Eruptives range in composition from the tholeiitic to calcalkalic basaltic lavas of Nishino-shima to the alkalic lavas of shoshonitic affinity on Iwo Jima [*Tsuya*, 1936; *Stern et al.*, 1984]. The arc is split at 24°N into the inactive or remnant West Mariana Ridge and the active Mariana Ridge, as a result of the opening of the Mariana Trough at 5 Ma [*Hussong and Uyeda*, 1981]. The volcanos of the Mariana Arc are inferred to postdate the opening of the Mariana Trough; those of the Volcano Arc may be as old as 20 Ma and postdate the opening of the Parece Vela-Shikoku Basin [*deVries Klein and Kobayashi*, 1980].

The Mariana active arc can be divided into three provinces based on the distribution of submarine and subaerial edifices [*Dixon and Stern*, 1983; *Stern et al.*, 1984, 1988*a*]. The Northern Seamount Province (NSP), from 24°N to 20°30'N and the Southern Seamount Province (SSP), from 16°30'N to Tracey Seamount at 13°20'N, are entirely submarine, whereas the Central Island Province (CIP), from Uracas at 20°30'N to Anatahan at 16°30'N, is largely subaerial but includes some submarine volcanos (Figure 1). Most of the edifices in the arc are constructed upon the juncture of older frontal arc crust and back-arc basin crust [*Hussong and Uyeda*, 1981; *Bloomer et al.*, 1989]. The older frontal arc crust, which is exposed on Guam and Saipan, includes boninites, arc tholeiitic basalts, andesites, and dacites of late Eocene through Miocene age [*Reagan and Meijer*, 1984; *Meijer*, 1980]. In both the CIP and NSP there are small chains of volcanos extending into the backarc basin from some of the edifices along the main magmatic front [*Hussong and Fryer*, 1983; *Bloomer et al.*, 1988]. These "cross-chains" may be associated with fractures or transforms in the backarc crust [*Hussong and Fryer*, 1983; *Fryer*, 1985].

The volcanos of the CIP have been studied extensively [*Meijer*, 1976, 1982; *Stern*, 1979; *Dixon and Batiza*, 1979; *Meijer and Reagan*, 1981, 1983; *Hole et al.*, 1984; *Stern and Ito*, 1983; *Woodhead and Fraser*, 1985]. The volcanos are erupting basalts to dacites of both the calcalkaline and tholeiitic series. The SSP has been described by *Dixon and Stern* [1983] and *Stern et al.* [1988a] and has erupted basalts, basaltic andesites, and dacites. The NSP has been described only at Fukujin [*Garcia et al.*, 1979; *Wood et al.*, 1981] and includes basaltic andesites and andesites.

Most of the andesitic lavas in the CIP and SSP result from low-pressure crystallization of a mantle-derived basaltic magma [*Stern*, 1979; *Meijer and Reagan*, 1981]. *Dixon and Stern* [1983] have suggested that a few of the lavas in the SSP may have been derived from dacitic parental melts.

*Dixon and Batiza* [1979] have noted that in the CIP a correlation exists between the size of a given edifice and the alkalinity of lavas erupted within it. Somewhat later, *Meijer and Reagan* [1983] suggested that each volcano may undergo an evolution from an early alkalic stage through a dominant tholeiitic stage to a late alkalic stage. The data reported here can be used to test these hypotheses.

## METHODS

The samples discussed here were recovered during cruise TT-192 of the R/V *Thomas Thompson* in November and December 1985. During this cruise, most of the previously unsampled submarine edifices in all three provinces of the Mariana Arc and the southern Volcano Arc were sampled and surveyed (Figure 1, Table 1), as were portions of the frontal arc, northern back-arc basin, and northern West Mariana Ridge. The edifices along the Mariana Arc can be classified as active (reported historical activity), dormant (very fresh rocks but no reported activity), extinct (altered rocks with Mn encrustations), or as frontal arc fragments (metavolcanics and several centimeter Mn crusts). A detailed description of the dredge recovery, classification of each edifice in the Mariana and Volcano Arcs, and bathymetric maps of the Mariana Ridge are reported by *Bloomer et al.* [1989]. Bathymetric maps of each edifice discussed here are included by *Lin et al.* (this issue).

We include in this discussion only active, dormant, or extinct edifices along the magmatic front of the active arc north of the island of Agrigan at 18°45'N. Excluded are rocks from frontal arc fragments and cross-chain volcanos. The former represent an older cycle of arc volcanism, and the latter may be influenced by backarc basin sources. Dredge locations and depths on each volcano discussed here are listed in Table 1.

All of the rock samples from each dredge haul were sorted aboard ship into petrographic categories, and representative samples of each volcanic or plutonic type were sawed for thin

*TABLE 1. Volcano Locations, Dredge Numbers and Depths, $SiO_2$ ranges, and Phenocryst Compositions for Submarine Volcanos in the Northern Mariana and Southern Volcano Arcs*

TABLE 1. Volcano Locations, Dredge Numbers and Depths, $SiO_2$ ranges, and Phenocryst Compositions for Submarine Volcanos in the Northern Mariana and Southern Volcano Arcs

| Volcano | Latitude | Activity | Petrography | $SiO_2$, % | n | D redge Hauls | Dredge Depths, m |
|---|---|---|---|---|---|---|---|
| CIP | | | | | | | |
| Poyo | 19°15' | extinct | PL-CPX-OL | 48.4 | 2 | D8 | 2800-2200 |
| Cheref | 19°25' | extinct | PL-CPX-OL-OPX-HB-OX | 49.5-64 | 8 | D9, 10, 11 | 900-605, 2100-1400, 1380-394 |
| Ascuncion | 19°42' | active | PL-CPX-OPX | | | | |
| Maug | 20°02' | extinct | PL-CPX | | | | |
| Supply Reef | 20°08' | dormant | PL-CPX | 53.8-59 | 3 | D13, 14 | 1650-1060, 1060-530 |
| Ahyi | 20°25' | dormant | PL-CPX-OPX-OL-OX | 48-53 | 3 | D15, 16 | 1930-1120, 1100-322 |
| Makhahnas | 20°28' | dormant | PL-CPX-OPX | 56.2-57.7 | 2 | D18 | 1190-950 |
| Uracas | 20°32' | active | PL-OPX-CPX | | | | |
| NW Uracas | 20°35' | extinct | PL-CPX-OPX | 51.7-52.4 | 2 | D19 | 1135-840 |
| SNSP | | | | | | | |
| Chammoro | 20°45' | dormant | PL-HB-OPX | 65.8 | 1 | D23 | 1600-1380 |
| South Daikoku | 21°03' | dormant | PL-CPX-OPX-HB | 54.3-61.8 | 6 | D25, 26 | 1450-1430, 850-500 |
| Daikoku | 21°20' | dormant | PL-OPX-CPX-OL | 59.1-63.3 | 4 | D29 | 920-400 |
| Eifuku | 21°25' | dormant | PL-CPX-OL-HB | 49.5-52.5 | 6 | D30, 31 | 975-725, 1715-1500 |
| Kasuga | 21°45' | extinct | PL-CPX-OPX | 56.8 | 1 | D33 | 1170-600 |
| Fukujin | 21°55' | active | PL-OPX-CPX | 52.7-55.4 | 3 | D34, 35 | 1600-1002, 1075-580 |
| Fukuyama | 22°23' | dormant | PL-CPX-OL-OPX | 52.5 | 1 | D38 | 1800-1740 |
| Shyoyo | 22°30' | extinct | PL-CPX-OPX | | | D41 | 1230-600 |
| Ichiyo | 23°00' | extinct | PL-CPX-OL-OPX | 53.2 | 1 | D44 | 2000-1760 |
| Nikko | 23°05' | active | PL-OL-CPX | 45.9-62 | 8 | D45, 46 | 1865-1310, 1470-1330 |
| NNSP | | | | | | | |
| Ko-Hiyoshi | 23°11' | dormant | PL-CPX-OL-OPX | 46.7-53.1 | 2 | D47 | 2030-1600 |
| South Hiyoshi | 23°15' | active | PL-OL-CPX | 50-56 | 9 | D48, 49 | 1230-740, 750-430 |
| Central Hiyoshi | 23°18' | dormant | PL-CPX-OL-HB | 48.8-51.8 | 5 | D51, 52 | 1400-1060, 1105-647 |
| North Hiyoshi | 23°22' | dormant | PL-CPX-OL-BI | 45.4-55.8 | 6 | D53, 54 | 1687-1280, 1640-1250 |
| Fukutoku | 23°33' | extinct | CPX-OL-PL | 48-52.6 | 6 | D55, 56, 57 | 1780-1070, 1500-1250, 1730-930 |
| SVA | | | | | | | |
| Minami Iwo Jima | 24°12' | extinct | CPX-OL-PL | | | | |
| Fukutoku-oka-no-ba | 24°18' | active | | | | | |
| Iwo Jima | 24°45' | active | PL-CPX-OL-HB | | | | |
| NVA | | | | | | | |
| Sin Kita Io Jima | 25°06' | extinct | PL-CPX-OL | 44-53.7 | 6 | D73 | 1620-1240 |
| Kita Iwo Jima | 25°30' | active | PL-CPX-OL | | | | |
| Kaitoku | 26°05' | active | PL-CPX-OL | 47.9-57.6 | 8 | D75, 77 | 1380-1090, 975-800 |
| Kaitaka | 26°40' | dormant | | | | | |
| Nishino Jima | 27°37' | active | PL-CPX | 51.2-56.4 | 11 | D79, 80, 82 | 1750-1735 |

Locations of the principal islands are included for reference. CIP is Central Island Province, SNSP is the southern Northern Seamount Province, NNSP is the northern Northern Seamount Province, SVA is the southern Volcano Arc, and NVA the northern Volcano Arc. The Alkalic Volcanic Province discussed in the text includes the NNSP and SVA. n indicates number of analyses from each edifice.

TABLE 2. Bulk Chemical and Petrographic Data for Lavas From the Northern Mariana and Volcano Arcs

| | Poyo | | Cheref | | | | | Supply Reef | | | Ahyi | | | Makhanas | | NW Uracas | |
|---|---|---|---|---|---|---|---|---|---|---|---|---|---|---|---|---|---|
| ID | D8:1,3 | | D9-6 | D9-20 | D10-2-7 | D10-2-11 | D10-1-2 | D13-11 | D14-15 | D13-22 | D16-3 | D15-3-3 | D15-3-2 | D18:9,11 | | D19:3-5,3-10 | |
| | av | sd | | | | | | | | | | | | av | sd | av | sd |
| $SiO_2$ | 48.34 | 0.12 | 53.54 | 51.30 | 55.65 | 49.50 | 63.98 | 53.79 | 55.76 | 59.30 | 47.79 | 52.95 | 52.78 | 56.99 | 0.73 | 52.11 | 0.31 |
| $TiO_2$ | 0.54 | 0.03 | 0.90 | 0.76 | 0.70 | 0.77 | 0.62 | 0.87 | 1.01 | 1.02 | 0.62 | 0.71 | 0.72 | 0.70 | 0.01 | 0.73 | 0.00 |
| $Al_2O_3$ | 15.36 | 0.39 | 17.88 | 18.37 | 18.33 | 21.83 | 17.14 | 19.59 | 17.11 | 18.62 | 14.31 | 18.11 | 17.19 | 17.73 | 0.28 | 18.36 | 0.26 |
| $FeO^t$ | 9.72 | 0.16 | 8.70 | 8.06 | 7.34 | 8.84 | 5.49 | 8.31 | 10.18 | 7.65 | 10.39 | 9.26 | 8.74 | 6.95 | 0.18 | 9.52 | 0.47 |
| MnO | 0.21 | 0.01 | 0.17 | 0.16 | 0.16 | 0.16 | 0.16 | 0.16 | 0.20 | 0.15 | 0.22 | 0.18 | 0.17 | 0.15 | 0.00 | 0.19 | 0.00 |
| MgO | 10.67 | 0.24 | 6.89 | 6.33 | 4.52 | 4.17 | 2.65 | 4.96 | 4.05 | 3.04 | 9.79 | 5.45 | 4.79 | 3.76 | 0.64 | 5.60 | 0.17 |
| CaO | 13.95 | 0.09 | 10.52 | 10.27 | 8.62 | 11.89 | 6.09 | 10.61 | 8.37 | 7.83 | 12.93 | 9.54 | 9.15 | 7.61 | 0.84 | 10.40 | 0.07 |
| $Na_2O$ | 1.34 | 0.06 | 2.36 | 2.23 | 2.64 | 1.98 | 3.28 | 2.65 | 2.94 | 3.51 | 1.68 | 2.85 | 2.80 | 2.96 | 0.23 | 2.12 | 0.05 |
| $K_2O$ | 0.21 | 0.01 | 0.74 | 0.63 | 0.61 | 0.55 | 1.22 | 0.40 | 0.44 | 0.68 | 0.37 | 0.57 | 0.70 | 1.21 | 0.10 | 0.39 | 0.01 |
| $P_2O_5$ | 0.13 | 0.07 | 0.13 | 0.10 | 0.08 | 0.11 | 0.15 | 0.14 | 0.12 | 0.16 | 0.09 | 0.05 | 0.08 | 0.13 | 0.03 | 0.16 | 0.06 |
| SUM | 100.46 | 0.61 | 100.02 | 98.21 | 98.65 | 99.80 | 100.78 | 101.48 | 100.18 | 101.96 | 98.19 | 99.67 | 97.12 | 98.16 | 0.32 | 99.56 | 0.64 |
| Rb | 8 | 3 | 14 | 12 | 18 | 14 | 25 | 8 | 16 | 12 | 15 | 18 | 12 | 20 | - | 11 | 3 |
| Sr | 219 | 14 | 281 | 320 | 230 | 295 | 318 | 264 | 206 | 229 | 277 | 190 | 295 | 330 | 15 | 266 | 12 |
| Ba | 46 | 0 | 137 | 169 | 173 | 110 | 261 | 160 | 151 | 242 | 98 | 170 | 201 | 218 | 2 | 146 | 13 |
| Zr | 23 | 0 | 65 | 60 | 66 | 47 | 91 | 54 | 62 | 88 | 34 | 44 | 64 | 76 | 7 | 45 | 3 |
| Y | 11 | 1 | 21 | 20 | 18 | 17 | 19 | 21 | 23 | 23 | 10 | 12 | 23 | 21 | 3 | 15 | 3 |
| Sc | 56 | | 43 | 43 | 34 | 34 | 16 | 36 | 40 | | | | 37 | 23 | 1 | 45 | |
| V | 289 | 13 | 297 | 288 | 235 | 334 | 126 | 306 | 367 | 218 | 286 | 198 | 262 | 178 | 16 | 319 | 22 |
| Cr | 314 | 12 | 117 | 79 | 43 | 8 | 12 | 63 | 20 | 9 | 283 | 39 | 30 | 24 | 9 | 23 | 1 |
| Ni | 104 | 0 | 47 | 40 | 37 | 11 | 10 | 24 | 14 | | | | 15 | 11 | 3 | 19 | |
| Cu | 87 | 1 | 104 | 32 | 101 | 89 | 24 | 120 | 173 | 170 | | | 84 | 28 | 8 | 140 | 6 |
| Texture | IS,G | | | S | G | | S | | IS | IS | | S,G | S,G | IS | | IS | |
| Alteration | N | | N | N | N | N | N | N | N | N | S | N | N | N | | N | N |
| Vesicles | 15 | | | | | 20 | | 10 | 15 | 5 | 20 | | | 20 | | | |
| OL | 20 | | 5 | | | 9 | | 3 | tr | 2 | 6 | tr | 2 | | | | |
| CPX | 10 | | 15 | 12 | 7 | 1 | | 10 | 1 | 5 | 19 | 9 | 10 | 4 | | 6 | |
| PL | 12 | | 23 | 18 | 20 | 30 | 27 | 13 | 9 | 10 | 13 | 30 | 25 | 19 | | 28 | |
| OPX | | | 2 | 8 | 3 | | 7 | 4 | | 3 | | 8 | 10 | 5 | | 6 | |
| HB | | | | | | | 8 | | | | | | | tr | | | |
| OX | | | | 2 | 1 | | 3 | | | | 2 | 3 | | 1 | | | |

TABLE 2. (continued)

| | Chamorro | South Daikoku | | | | | | Daikoku | | | | Eifuku | | | | | |
|---|---|---|---|---|---|---|---|---|---|---|---|---|---|---|---|---|---|
| ID | D23-3 | D25-8 | D25-18 | D26:4-5,4-6 | | D25-1 | D26-3-1 | D29:1-1,1-2 | | D29:2-2,2-3 | | D31-1-6 | D31-1-4 | D30:7,8 | | D30-6 | D31-2-2 |
| | | | | av | sd | | | av | sd | av | sd | | | av | sd | | |
| $SiO_2$ | 65.81 | 54.33 | 56.53 | 59.49 | 0.76 | 58.19 | 61.80 | 59.49 | 0.42 | 62.88 | 0.38 | 49.05 | 49.63 | 51.02 | 0.52 | 52.53 | 52.54 |
| $TiO_2$ | 0.44 | 1.01 | 1.00 | 0.81 | 0.01 | 0.94 | 0.70 | 0.75 | 0.02 | 0.80 | 0.00 | 0.78 | 0.76 | 0.80 | 0.01 | 0.85 | 1.01 |
| $Al_2O_3$ | 15.61 | 17.11 | 16.57 | 16.64 | 0.19 | 16.39 | 16.86 | 15.68 | 0.45 | 16.37 | 0.18 | 13.78 | 14.57 | 17.09 | 0.50 | 17.68 | 19.92 |
| $FeO^t$ | 4.17 | 9.19 | 10.29 | 8.10 | 0.25 | 8.89 | 6.68 | 6.99 | 0.17 | 6.78 | 0.01 | 9.71 | 9.54 | 9.69 | 0.24 | 9.82 | 10.21 |
| MnO | 0.13 | 0.19 | 0.19 | 0.20 | 0.00 | 0.19 | 0.18 | 0.16 | 0.00 | 0.16 | 0.00 | 0.20 | 0.18 | 0.18 | 0.00 | 0.18 | 0.19 |
| MgO | 2.08 | 4.47 | 3.20 | 2.43 | 0.16 | 2.01 | 1.67 | 3.59 | 0.05 | 2.29 | 0.05 | 8.78 | 7.67 | 6.11 | 0.04 | 5.62 | 3.72 |
| CaO | 5.08 | 9.30 | 7.06 | 6.00 | 0.09 | 5.49 | 6.28 | 6.12 | 0.16 | 5.38 | 0.04 | 12.05 | 11.76 | 10.20 | 0.25 | 10.52 | 9.37 |
| $Na_2O$ | 3.46 | 2.96 | 3.29 | 3.91 | 0.04 | 3.95 | 3.87 | 3.63 | 0.07 | 3.87 | 0.03 | 1.92 | 2.25 | 2.46 | 0.16 | 2.42 | 2.83 |
| $K_2O$ | 1.32 | 0.70 | 1.06 | 0.96 | 0.04 | 1.50 | 0.92 | 1.87 | 0.00 | 2.05 | 0.01 | 0.87 | 0.93 | 1.28 | 0.06 | 0.95 | 1.31 |
| $P_2O_5$ | 0.09 | 0.09 | 0.19 | 0.18 | 0.00 | 0.18 | 0.23 | 0.22 | 0.02 | 0.23 | 0.01 | 0.10 | 0.14 | 0.19 | 0.01 | 0.19 | 0.20 |
| SUM | 98.19 | 99.35 | 99.38 | 98.59 | 0.76 | 97.73 | 99.18 | 98.49 | 0.31 | 100.79 | 0.50 | 97.24 | 97.43 | 99.00 | 0.37 | 100.76 | 101.30 |
| Rb | 20 | 12 | 18 | 20 | 4 | 28 | 15 | 36 | 0 | 40 | 0 | 17 | 26 | 23 | 3 | 20 | 24 |
| Sr | 295 | 308 | 316 | 378 | 4 | 382 | 412 | 369 | 6 | 390 | 22 | 537 | 386 | 756 | 25 | 578 | 785 |
| Ba | 424 | 211 | 336 | 342 | 10 | 370 | 350 | 486 | 25 | 527 | 34 | 277 | 190 | 424 | 8 | 286 | 442 |
| Zr | 55 | 67 | 112 | 109 | 1 | 110 | 94 | 93 | 6 | 143 | 11 | 46? | 18 | 78 | 7 | 58 | 46 |
| Y | 17 | 25 | 26 | 27 | 0 | 31 | 25 | 27 | 1 | 28 | 1 | 14 | 19 | 15 | 1 | 19 | 19 |
| Sc | 14 | 38 | | 30 | 2 | | | 26 | 3 | 24 | 2 | | 47 | 18 | 18 | 36 | 26 |
| V | 90 | 274 | 259 | 114 | 6 | 88 | 92 | 128 | 3 | 124 | 1 | 299 | 187 | 320 | 7 | 256 | 338 |
| Cr | 6 | 15 | 0 | 11 | 6 | 11 | 2 | 96 | 11 | 22 | 3 | 225 | 120 | 79 | 5 | 69 | 15 |
| Ni | 5 | 8 | | 4 | 0 | | | 31 | 0 | 7 | 0 | | 52 | 31 | 0 | 21 | 14 |
| Cu | 8 | 121 | 196 | 53 | 1 | 76 | 48 | 44 | 3 | 37 | 5 | 139 | 106 | 149 | 18 | 127 | 183 |
| Texture | IS | IS,S | IS,G | IS,G,F | | IS | IS,G | P | | T | | | IS,IG,X | IS,IG | | | IS |
| Alteration | | N | N | N | | N | N | N | | N | | N,G | N | N,G | | N,G | N,G |
| Vesicles | 20 | 30 | 8 | 2-20 | | 30 | 12 | 5 | | 8 | | 20 | 5 | 5 | | 15 | 2 |
| OL | | | | | | | | 0-0.5 | | | | 2 | 2 | 3 | | 2 | 1 |
| CPX | (2 QTZ) | 5 | 2 | 2-3 | | 2 | 1 | 1.5-5 | | 5 | | 10 | 8 | 6 | | 5 | 1 |
| PL | 20 | 20 | 5 | 10 | | 2 | 20 | 2-6 | | 8 | | 5 | 10 | 12 | | 11 | 9 |
| OPX | 1 | 5 | | 0-2 | | | 1 | 0.2-1 | | 1 | | | | | | | |
| HB | 10 | | | | | | | | | | | | | | | | |
| OX | 2 | | | <1 | | | <1 | | | 1 | | | | | | | |

TABLE 2. (continued)

| | Kasuga | Fukujin | | | Fukuyama | Ichiyo | Nikko | | | | | | | Ko-Hiyoshi | |
|---|---|---|---|---|---|---|---|---|---|---|---|---|---|---|---|
| ID | D33-3-1 | D34-2-2 | D34-1-2 | D35-1-2 | D38-2 | D44-1-5 | D46-5-1 | D45-8 | D45:3;D46:1-1,3-1 av | D45:3;D46:1-1,3-1 sd | D45-1 | D45-2 | D45-11 | D47-1-5 | D47-1-1 |
| $SiO_2$ | 56.77 | 53.11 | 52.69 | 55.40 | 52.50 | 53.21 | 45.76 | 47.70 | 46.61 | 0.89 | 51.62 | 49.93 | 61.71 | 46.66 | 53.06 |
| $TiO_2$ | 0.51 | 0.85 | 0.90 | 0.97 | 0.54 | 0.73 | 0.82 | 0.87 | 0.87 | 0.03 | 1.02 | 0.77 | 0.89 | 0.86 | 0.79 |
| $Al_2O_3$ | 17.37 | 18.71 | 20.82 | 18.50 | 16.48 | 17.79 | 19.14 | 16.98 | 19.99 | 1.00 | 17.37 | 17.91 | 15.23 | 20.92 | 21.73 |
| $FeO^t$ | 7.81 | 9.56 | 8.32 | 7.96 | 8.89 | 8.62 | 9.67 | 12.10 | 10.78 | 0.40 | 11.75 | 10.05 | 5.68 | 9.37 | 7.17 |
| MnO | 0.17 | 0.17 | 0.14 | 0.15 | 0.17 | 0.19 | 0.19 | 0.20 | 0.18 | 0.00 | 0.21 | 0.17 | 0.18 | 0.17 | 0.14 |
| MgO | 4.44 | 4.10 | 3.25 | 3.24 | 8.94 | 3.81 | 7.20 | 6.45 | 5.35 | 0.29 | 4.93 | 4.75 | 1.24 | 3.94 | 2.88 |
| CaO | 8.95 | 9.41 | 11.27 | 8.83 | 11.26 | 8.94 | 13.74 | 11.74 | 11.68 | 0.89 | 10.76 | 11.08 | 4.10 | 12.52 | 9.09 |
| $Na_2O$ | 2.33 | 2.48 | 2.22 | 2.64 | 1.40 | 2.88 | 1.88 | 2.02 | 2.19 | 0.09 | 2.47 | 2.22 | 4.53 | 2.44 | 3.62 |
| $K_2O$ | 0.38 | 1.19 | 1.01 | 1.27 | 0.31 | 1.23 | 0.26 | 0.30 | 0.34 | 0.01 | 0.23 | 0.26 | 1.51 | 0.79 | 1.88 |
| $P_2O_5$ | 0.02 | 0.20 | 0.14 | 0.17 | 0.09 | 0.13 | 0.09 | 0.06 | 0.09 | 0.02 | 0.12 | 0.07 | 0.21 | 0.56 | 0.54 |
| SUM | 98.75 | 99.78 | 100.76 | 99.13 | 100.63 | 97.53 | 98.75 | 98.42 | 98.09 | 0.63 | 100.48 | 97.21 | 95.28 | 98.23 | 100.90 |
| Rb | 8 | 28 | 21 | 29 | | | | | | | | | | 12 | 35 |
| Sr | 236 | 445 | 469 | 388 | 11 | 21 | 4 | 5 | 6 | 0 | 3 | 4 | 27 | 940 | 1192 |
| Ba | 205 | 320 | 328 | 496 | 266 | 411 | 392 | 286 | 424 | 53 | 322 | 372 | 302 | 450 | 830 |
| Zr | 33 | 62 | 68 | 97 | 173 | 384 | 117 | 93 | 159 | 7 | 148 | 151 | 667 | 30 | 65 |
| Y | 14 | 18 | 15 | 22 | 32 | 71 | 24 | 18 | 38 | 6 | 42 | 42 | 197 | 30 | 25 |
| Sc | | 42 | | 40 | 10 | 26 | 11 | 9 | 13 | 2 | 20 | 29 | 40 | 26 | 16 |
| V | 228 | 300 | 308 | 284 | 50 | 31 | 41 | 43 | 33 | 9 | 44 | 43 | 14 | 360 | 220 |
| Cr | | 34 | 29 | 18 | 296 | 233 | 302 | 321 | 359 | 12 | 348 | 363 | 58 | 12 | 4 |
| Ni | | | | | 208 | 17 | 58 | 8 | 16 | 3 | 9 | 27 | 1 | 13 | 2 |
| Cu | 42 | 137 | 145 | 155 | 67 | 7 | 40 | 13 | 28 | 6 | 17 | 18 | | 170 | 129 |
| Texture | P,S | P | IS | IG | 116 | 128 | 121 | 112 | 134 | 30 | 128 | 148 | 14 | | |
| Alteration | S | N | S | S | IG,IS,X | IS | IG,IS,X | IS,IG | P | G | G,IG | G | PI | GG | P,G |
| Vesicles | | 2 | 2 | <1 | S | N,G | M* | S* | M* | M* | S* | M * | M* | M* | M* |
| OL | | | | | 5 | <1 | 5 | 17 | 40 | 10-60 | 15 | 20 | 30 | 35 | 15 |
| CPX | 5 | 3 | 3 | 2 | 1 | | 3 | 1 | 7 | 1-6 | 1 | 1 | | 1 | 1 |
| PL | 10 | 11 | 20 | 10 | 8 | 6 | 5 | 4 | | 1-5 | 3 | 5 | 3 | 25 | 3 |
| OPX | | 3 | 1 | | 10 | 10 | 18 | 25 | 17 | 10-20 | 22 | 30 | 12 | tr | 30 |
| HB | | | | | 3 | 2 | | | | | 1 | | tr | | |
| OX | | | | | 1 | | | | | | | | | | 2 |

TABLE 2. (continued)

| | South Hiyoshi | | | | | | Central Hiyoshi | | | | | North Hiyoshi | | | | |
|---|---|---|---|---|---|---|---|---|---|---|---|---|---|---|---|---|
| ID | D48:1-4;D49:1-2, 3-2, D49:4-3,5-2,PB | | D48-1-2 | D48-2-3 | D48-1-1 | D49-2-1 | D52:1-1,1-4,1-5 | | D52-3-1 | D51-3 | D52-3-2 | D54-1-3 | D54:1-1,1-4 | | D53:1-2,1-3 | |
| | av | sd | | | | | av | sd | | | | | av | sd | av | sd |
| $SiO_2$ | 50.68 | 0.51 | 53.10 | 56.20 | 54.51 | 54.94 | 50.25 | 0.00 | 51.86 | 51.84 | 50.80 | 45.34 | 45.79 | 0.52 | 55.60 | 0.21 |
| $TiO_2$ | 0.98 | 0.03 | 1.04 | 1.12 | 0.81 | 0.90 | 0.80 | 0.01 | 0.75 | 1.03 | 0.71 | 0.97 | 1.01 | 0.03 | 0.66 | 0.01 |
| $Al_2O_3$ | 18.74 | 0.41 | 16.66 | 16.93 | 19.77 | 17.24 | 18.54 | 0.07 | 19.10 | 20.06 | 20.32 | 17.97 | 18.52 | 0.15 | 18.72 | 0.26 |
| $FeO^t$ | 8.97 | 0.28 | 10.14 | 9.60 | 6.57 | 7.91 | 8.54 | 0.30 | 8.15 | 8.60 | 7.55 | 10.28 | 10.82 | 0.15 | 6.57 | 0.06 |
| MnO | 0.18 | 0.01 | 0.20 | 0.22 | 0.14 | 0.22 | 0.21 | 0.01 | 0.22 | 0.21 | 0.20 | 0.20 | 0.18 | 0.00 | 0.15 | 0.00 |
| MgO | 3.33 | 0.23 | 3.02 | 2.50 | 2.47 | 2.16 | 4.23 | 0.10 | 3.29 | 3.18 | 3.15 | 6.72 | 6.43 | 0.54 | 2.83 | 0.00 |
| CaO | 8.79 | 0.27 | 6.68 | 6.05 | 9.61 | 5.23 | 9.31 | 0.26 | 8.94 | 8.70 | 9.00 | 11.75 | 11.56 | 0.18 | 6.67 | 0.09 |
| $Na_2O$ | 3.48 | 0.14 | 3.79 | 4.13 | 2.91 | 4.19 | 2.97 | 0.09 | 3.62 | 3.32 | 3.38 | 2.27 | 2.32 | 0.09 | 4.00 | 0.30 |
| $K_2O$ | 2.07 | 0.13 | 2.85 | 3.57 | 2.26 | 3.45 | 2.54 | 0.08 | 2.23 | 1.28 | 1.59 | 1.17 | 1.40 | 0.02 | 4.49 | 0.07 |
| $P_2O_5$ | 0.29 | 0.03 | 0.42 | 0.51 | 0.25 | 0.41 | 0.34 | 0.01 | 0.28 | 0.26 | 0.28 | 0.33 | 0.28 | 0.03 | 0.26 | 0.00 |
| SUM | 97.51 | 1.55 | 97.90 | 100.83 | 99.30 | 96.65 | 97.74 | 0.46 | 98.44 | 98.45 | 96.98 | 96.96 | 98.31 | 0.81 | 99.92 | 0.69 |
| Rb | 48 | 3 | 71 | 94 | 53 | 88 | 63 | 2 | 53 | 31 | 32 | 24 | 26 | 4 | 158 | 48 |
| Sr | 674 | 45 | 528 | 557 | 671 | 547 | 1070 | 25 | 944 | 938 | 999 | 1062 | 1134 | 4 | 988 | 16 |
| Ba | 672 | 21 | 877 | 1377 | 622 | 983 | 837 | 18 | 741 | 615 | 626 | 417 | 714 | 32 | 818 | 14 |
| Zr | 88 | 7 | 167 | 142 | 74 | 132 | 68 | 16 | 58 | 70 | 53 | 34 | 31 | 4 | 164 | 13 |
| Y | 25 | 4 | 33 | 40 | 25 | 40 | 21 | 1 | 18 | 24 | 23 | 21 | 21 | 1 | 23 | 2 |
| Sc | 23 | 1 | 19 | 21 | 22 | 19 | 21 | 1 | 19 | 13 | 17 | 40 | 35 | 0 | 15 | 1 |
| V | 260 | 29 | 204 | 222 | 172 | 116 | 271 | 2 | 211 | 221 | 203 | 360 | 398 | 2 | 198 | 11 |
| Cr | 11 | 4 | 7 | 5 | 27 | 8 | 9 | 2 | 20 | 17 | 10 | 54 | 49 | 2 | 18 | 1 |
| Ni | 17 | 4 | 4 | 6 | 11 | 3 | 11 | 6 | 8 | 5 | 15 | 39 | 30 | 2 | 11 | 3 |
| Cu | 192 | 21 | 250 | 209 | 107 | 82 | 88 | 25 | 110 | 159 | 49 | 184 | 166 | 16 | 122 | 9 |
| Texture | IG,G | | P | | | T | IG,IS,G | | | | | IG,IS | IG,IS | | P,G,IS | |
| Alteration | M | | N | S* | M | N | N | | S | | S | S | S | | N,S | |
| Vesicles | 10-40 | | <1 | 50 | | | | | 9 | | 6 | 10 | 10 | | | |
| OL | 1-3 | | 1 | 1 | 1 | tr | 1-2 | | 1 | | 1 | 3 | 4 | | 3 | |
| CPX | 1-3 | | 5 | | 13 | 1 | 10-25 | | 4 | | 5 | 4 | 5 | | 5 | |
| PL | 10-17 | | 8 | 12 | 25 | 2 | 20-25 | | 20 | | 22 | 11 | 10 | | 20 | |
| OPX | | | | | | | | | tr | | | | | | (3 BIO) | |
| HB | | | | | | | tr | | | | | | | | | |
| OX | | | 1 | | | | 2-7 | | 1 | | <1 | tr | <1 | | 3 | |

TABLE 2. (continued)

| | Fukutoku | | | | | Fukutoku-oka-no-ba | | | S. Kita Iwo Jima | | | | |
|---|---|---|---|---|---|---|---|---|---|---|---|---|---|
| ID | D56-1 | D57:5,6 | | D55-1-2 | D55-1-1 | Yoshida et al. 1987 | | | D73-2-1 | D73-4-4 | D73-2-3 | D73-2-2 | D73-4-2 |
| | | av | sd | | | av | sd | | | | | | |
| $SiO_2$ | 48.80 | 48.33 | 0.30 | 48.83 | 52.56 | 60.88 | 0.80 | 60.82 | 43.36 | 47.39 | 45.96 | 46.41 | 53.67 |
| $TiO_2$ | 0.77 | 0.74 | 0.02 | 0.80 | 0.73 | 0.55 | 0.02 | 0.45 | 0.65 | 0.70 | 0.74 | 0.52 | 0.62 |
| $Al_2O_3$ | 16.12 | 15.35 | 0.25 | 15.64 | 19.52 | 16.43 | 0.24 | 16.63 | 15.29 | 18.98 | 19.96 | 21.40 | 19.74 |
| $FeO^t$ | 10.00 | 10.26 | 0.11 | 7.62 | 8.75 | 4.52 | 0.17 | 4.50 | 10.15 | 11.05 | 10.45 | 9.95 | 7.11 |
| MnO | 0.33 | 0.27 | 0.08 | 0.16 | 0.16 | 0.17 | 0.00 | 0.39 | 0.20 | 0.20 | 0.21 | 0.18 | 0.19 |
| MgO | 9.12 | 7.75 | 0.06 | 7.64 | 5.43 | 1.96 | 0.28 | 1.79 | 12.04 | 7.19 | 6.97 | 6.06 | 2.82 |
| CaO | 12.07 | 12.32 | 0.04 | 11.01 | 9.71 | 3.49 | 0.15 | 3.35 | 14.15 | 12.51 | 12.23 | 13.89 | 7.71 |
| $Na_2O$ | 1.65 | 2.27 | 0.07 | 1.99 | 2.25 | 5.38 | 0.34 | 5.12 | 1.16 | 2.02 | 1.88 | 1.66 | 3.66 |
| $K_2O$ | 1.00 | 1.17 | 0.06 | 2.51 | 1.45 | 4.39 | 0.16 | 4.64 | 0.31 | 0.46 | 0.48 | 0.44 | 1.46 |
| $P_2O_5$ | 0.16 | 0.21 | 0.01 | 0.41 | 0.19 | 0.19 | 0.01 | 0.19 | 0.08 | 0.08 | 0.08 | 0.09 | 0.12 |
| SUM | 100.02 | 98.65 | | 96.61 | 100.75 | 97.96 | | 97.88 | 97.39 | 100.58 | 97.96 | 100.60 | 97.10 |
| Rb | 19 | 17 | 2 | 77 | 29 | 95 | 3 | | 4 | 6 | 6 | 6 | 17 |
| Sr | 663 | 781 | 13 | 984 | 886 | 447 | 1 | | 432 | 360 | 590 | 611 | 854 |
| Ba | 343 | 529 | 20 | 605 | 628 | 1570 | 20 | | 89 | 105 | 155 | 146 | 345 |
| Zr | 33 | 62 | 23 | 67 | 84?? | 251 | 6 | | 11 | 6 | 36 | 19 | 64 |
| Y | 13 | 13 | 0 | 20 | 14 | 31 | 1 | | 9 | 12 | 12 | 12 | 20 |
| Sc | 46 | 41 | 6 | 34 | 35 | 11 | 1 | | 26 | 35 | 42 | 43 | 22 |
| V | 295 | 263 | 3 | 247 | 270 | | | | 369 | 174 | 306 | 348 | 159 |
| Cr | 218 | 143 | 6 | 199 | 41 | 35 | 3 | | 166 | 22 | 36 | 41 | 17 |
| Ni | 68 | 86 | 30 | 42 | 18 | 12 | 1 | | 22 | 11 | 25 | 24 | 11 |
| Cu | 110 | 146 | 13 | 92 | 93 | | | | 90 | 71 | 123 | 120 | 68 |
| Texture | | P,G | P | IS,IG,G | G | | | | P | | | | P,G |
| Alteration | S | N | S | S | S | | | | S | N | N | N | N |
| Vesicles | 20 | 15 | 15 | 10 | 20 | | | | 15 | 10 | 20 | | 10 |
| OL | 3 | 2 | 1 | 3 | 2 | | | | 1 | | 1 | | |
| CPX | 20 | 13 | 5 | 30 | 10 | | | | 15 | 1 | 9 | | 1 |
| PL | 15 | | | 20 | 27 | | | | | 2 | 11 | 30 | 15 |
| OPX | | | | tr | tr | | | | tr | | | | |
| HB | | | | | | | | | | | | | |
| OX | | | | | | | | | | | | | |

TABLE 2. (continued)

TABLE 2. (continued)

| ID | Kaitoku | | | | | Nishino Jima | | | | | | | Estimated one sigma errors |
|---|---|---|---|---|---|---|---|---|---|---|---|---|---|
| | D77-13 | D77-5 | D77-1 | D75:4,8 | | D79:1,2,6 | | D80:1,2,3,6 | | D80-4 | D79:3,7 | | |
| | | | | av | sd | av | sd | av | sd | | av | sd | |
| $SiO_2$ | 47.94 | 55.20 | 55.55 | 57.06 | 0.81 | 52.16 | 1.02 | 52.55 | 0.90 | 51.77 | 56.43 | 0.01 | 0.60 |
| $TiO_2$ | 0.72 | 0.69 | 1.30 | 1.10 | 0.00 | 0.70 | 0.02 | 0.72 | 0.04 | 0.71 | 0.73 | 0.04 | 0.06 |
| $Al_2O_3$ | 18.78 | 18.12 | 15.14 | 14.98 | 0.01 | 19.01 | 0.17 | 17.08 | 0.36 | 17.34 | 17.43 | 0.59 | 0.30 |
| $FeO^t$ | 9.97 | 7.82 | 10.14 | 10.03 | 0.15 | 9.72 | 0.15 | 8.92 | 0.32 | 8.68 | 7.83 | 0.16 | 0.20 |
| MnO | 0.17 | 0.22 | 0.22 | 0.26 | 0.01 | 0.18 | 0.01 | 0.19 | 0.01 | 0.18 | 0.17 | 0.00 | 0.02 |
| MgO | 7.92 | 3.32 | 2.62 | 2.36 | 0.13 | 5.29 | 0.12 | 5.20 | 0.17 | 5.18 | 3.74 | 0.28 | 0.15 |
| CaO | 13.97 | 7.68 | 6.66 | 6.15 | 0.09 | 10.06 | 0.12 | 9.47 | 0.19 | 9.62 | 8.29 | 0.11 | 0.20 |
| $Na_2O$ | 1.61 | 3.98 | 3.85 | 4.18 | 0.08 | 2.31 | 0.13 | 2.39 | 0.05 | 2.41 | 2.76 | 0.08 | 0.10 |
| $K_2O$ | 0.16 | 0.65 | 1.03 | 1.15 | 0.02 | 0.40 | 0.02 | 0.44 | 0.03 | 0.46 | 0.63 | 0.05 | 0.05 |
| $P_2O_5$ | 0.08 | 0.07 | 0.17 | 0.18 | 0.01 | 0.06 | 0.02 | 0.09 | 0.02 | 0.06 | 0.06 | 0.01 | 0.04 |
| SUM | 101.32 | 97.75 | 96.68 | 97.44 | 0.84 | 99.87 | 1.33 | 97.05 | 0.46 | 96.41 | 98.05 | | 0.76 |
| Rb | 8 | 7 | 15 | 16 | 0 | 6 | 0 | 6 | 0 | 6 | 8 | 0 | 1 |
| Sr | 243 | 363 | 259 | 251 | 1 | 160 | 6 | 158 | 2 | 112 | 197 | 6 | 5% |
| Ba | 42 | 156 | 232 | 252 | 3 | 130 | 5 | 138 | 5 | 105 | 172 | 1 | 5% |
| Zr | 19 | 59 | 122 | 105 | 17 | 53 | 6 | 58 | 3 | | 81 | 8 | 10 |
| Y | 11 | 22 | 32 | 39 | 2 | 20 | 3 | 23 | 0 | 22 | 26 | 0 | 1 |
| Sc | 52 | 24 | 25 | 26 | 2 | 39 | 3 | 41 | 1 | 29 | 34 | 2 | 1 |
| V | 309 | 124 | 200 | 155 | 11 | 276 | 24 | 254 | 19 | 200 | 215 | 10 | 10 |
| Cr | 68 | 6 | <10 | 12 | 2 | 48 | 10 | 32 | 7 | 33 | 19 | 6 | 9 |
| Ni | 47 | 6 | 12 | 6 | 1 | 16 | 2 | 17 | 2 | 10 | 15 | 0 | 4 |
| Cu | 99 | 46 | 109 | 63 | 3 | 85 | 27 | 135 | 13 | 104 | 51 | 3 | 5 |
| Texture | IG,IS | P | | P | | IG,G | | IG,IS | | IG,IS | G | | |
| Alteration | S | N | M | N | | S,M | | N | | N | S* | | |
| Vesicles | 8 | 15 | | | | | | 20-25 | | 20 | 10-30 | | |
| OL | | 1 | 5 | | | 1-3 | | | | | 1 | | |
| CPX | 2 | 7 | 5 | 1 | | 8-15 | | 5-10 | | 5 | 10 | | |
| PL | 20 | 30 | 25 | 5 | | 12-25 | | 10-20 | | 10 | 22 | | |
| OPX | | | | | | 0-2 | | 2-3 | | 1 | tr | | |
| HB | | | | | | | | | | | | | |
| OX | | 2 | | | | 2-3 | | tr | | tr | | | |

Errors in the last column are estimated from standard deviations of replicate analyses (over three years) of an EPR basalt and a southern California dacite and replicate analyses of USGS standards. Errors on Zr, V, and Cr are high as these analyses were done on dilute solutions of fused glasses. Table is arranged from the southernmost volcano to the northernmost. av indicates an average of several samples; sd the standard deviation of that average. Samples numbers are listed for individual and averaged samples. Mineral and vesicle proportions are from visual modes. PL is plagioclase, OL olivine, CPX clinopyroxene, OPX orthopyroxene, AM amphibole, OX titanomagnetite, QTZ quartz, and BIO biotite. tr indicates a trace amount of the mineral is present. In alteration row N is none, S is slight, M is moderate. All iron is calculated as FeO. In the texture row notable textural features are included: IG is intergranular groundmass, IS intersertal, G glomerophyric, X indicates the presence of cognate or lithic xenoliths, S is felty, T trachytic. Analyses do not include volatiles, and so commonly sum below 100%. The one sigma errors on the sums is ±0.8%.

* The "alteration" is principally a green clay filling vesicles.

section preparation and chemical analysis. Slabs for chemical analysis were cleaned of saw marks with a diamond lap, boiled in deionized water, rinsed and dried, then crushed in a ceramic surfaced jaw crusher and powdered in WC canisters in a swing mill. Splits of 0.1 g were fused with 0.7 g of a lithium borate flux and dissolved in 100 mL of 2% $HNO_3$. Major and trace (Ba, Sr, Zr, Cu, V, Cr, Rb) elements were determined on these solutions by plasma and flame emission spectrometry using U.S. Geological Survey (USGS) reference materials and multielement aqueous standards for calibration. Y, Sc, and Ni were determined on solutions of 0.5 g rock dissolved in HF acid and diluted to 50 ml with 10% $HNO_3$. Analyses that were nearly identical were combined (as they are assumed to be of pieces of the same unit) and means, standard deviations, and the sample numbers used in the averages are reported for each (Table 2). The latter are provided for reference to other data sets on these samples [*Lin et al.*, this issue].

Analyses of volcanic rocks from Agrigan, Pagan, Ascuncion and Uracas [*Stern*, 1979; *Dixon and Batiza*, 1979; *Kuno*, 1962] in the Mariana Arc and Iwo Jima [*Stern et al.*, 1984; *Tsuya*, 1936], Minami-Iwo Jima [*Yuasa and Tamaki*, 1982], and Fukutoku-oka-no-ba [*Yoshida et al.*, 1987] in the Volcano Arc are included in some of the figures for comparison.

Phenocryst mineral compositions were determined using a nine-channel automated American Research Laboratories electron probe at Virginia Polytechnic and State University in Blacksburg, Virginia. Standardization was by reference to materials from the Smithsonian Institution and the USGS, using a Bence-Albee correction. Beam current was maintained at 10 na, count times were 10 to 20 s, and the average spot size was 10 microns.

## Results

The dredge hauls from the submarine volcanos recovered a diverse suite of samples including siltstones, volcanoclastic siltstones, volcanic breccias, gabbroic xenoliths, pumices, and volcanic rocks ranging in composition from basalt to dacite. Volcanic rocks within single hauls are either very uniform in composition (Table 1, Makhahnas) or cover a substantial range of $SiO_2$ (Table 1, 9% in South Kita Iwo Jima).

### *Petrographic Characteristics*

The volcanic rock samples are typically densely phyric (commonly 10-30%, to as high as 50%, Table 2) with glomerophyric and seriate porphyritic textures. The samples are usually vesicular (5-30%, Table 2) and most are very fresh (Table 2). Slight alteration of glassy groundmass to smectites oocurs in some and some of the NSP lavas have a green clay filling some vesicles. Olivines are commonly slightly oxidized and veined with iddingsite.

Phenocryst assemblages are generally anhydrous and are dominated by plagioclase (PLAG). The typical phenocryst assemblages in these rocks are plagioclase, clinopyroxene, orthopyroxene, ± titanomagnetite; plagioclase, clinopyroxene, olivine ± titanomagnetite ± orthopyroxene; and plagioclase, clinopyroxene, ± titanomagnetite (Table 2). The PLAG is often zoned with glass inclusions along zone boundaries and may have clear rims overgrown on the corroded cores. PLAG commonly occurs in glomerocrysts with pyroxenes and titanomagnetites.

Orthopyroxene (OPX), clinopyroxene (CPX), and olivine (OL) all occur in these lavas but their relative abundances vary greatly. OL is most common (2-10%) in the southernmost edifices (Poyo to Ahyi), is largely absent between Uracas and Eifuku, and occurs variously (1-6%) in the volcanos north of Eifuku. It occurs as both euhedral phenocrysts and as subrounded grains with rims of orthopyroxene or clinopyroxene.

Orthopyroxene occurs in the CIP and southern NSP (1-10%), is absent in most of the NSP, particularly the Hiyoshi Seamounts, and reappears in small amounts in the Volcano Arc north of Iwo Jima. It most commonly occurs as small to medium euhedral crystals or in glomerocrysts.

CPX is usually the second most abundant phenocryst

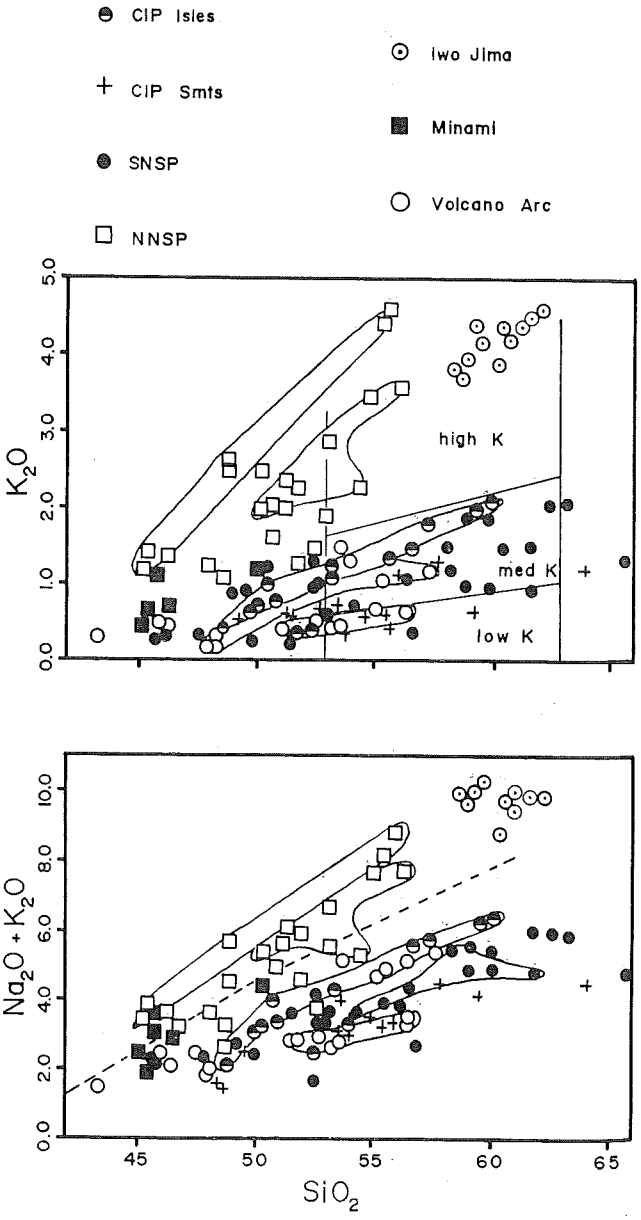


Fig. 2. Geochemical variations in arc lavas from the Mariana and Volcano arcs. Data sources for the islands are noted in the text. Low-, medium-, and high-K fields from *Gill* [1981]. Dotted line in lower figure divides alkalic rocks (upper half) from subalkalic rocks (lower half)[after *Irvine and Baragar*, 1971]. Fields for samples from individual volcanos are enclosed in thin lines. Points labeled Iwo Jima include anlayses from Fukutoku-oka-noba, a small active seamount adjacent to Iwo Jima [*Yoshida et al.*, 1987].

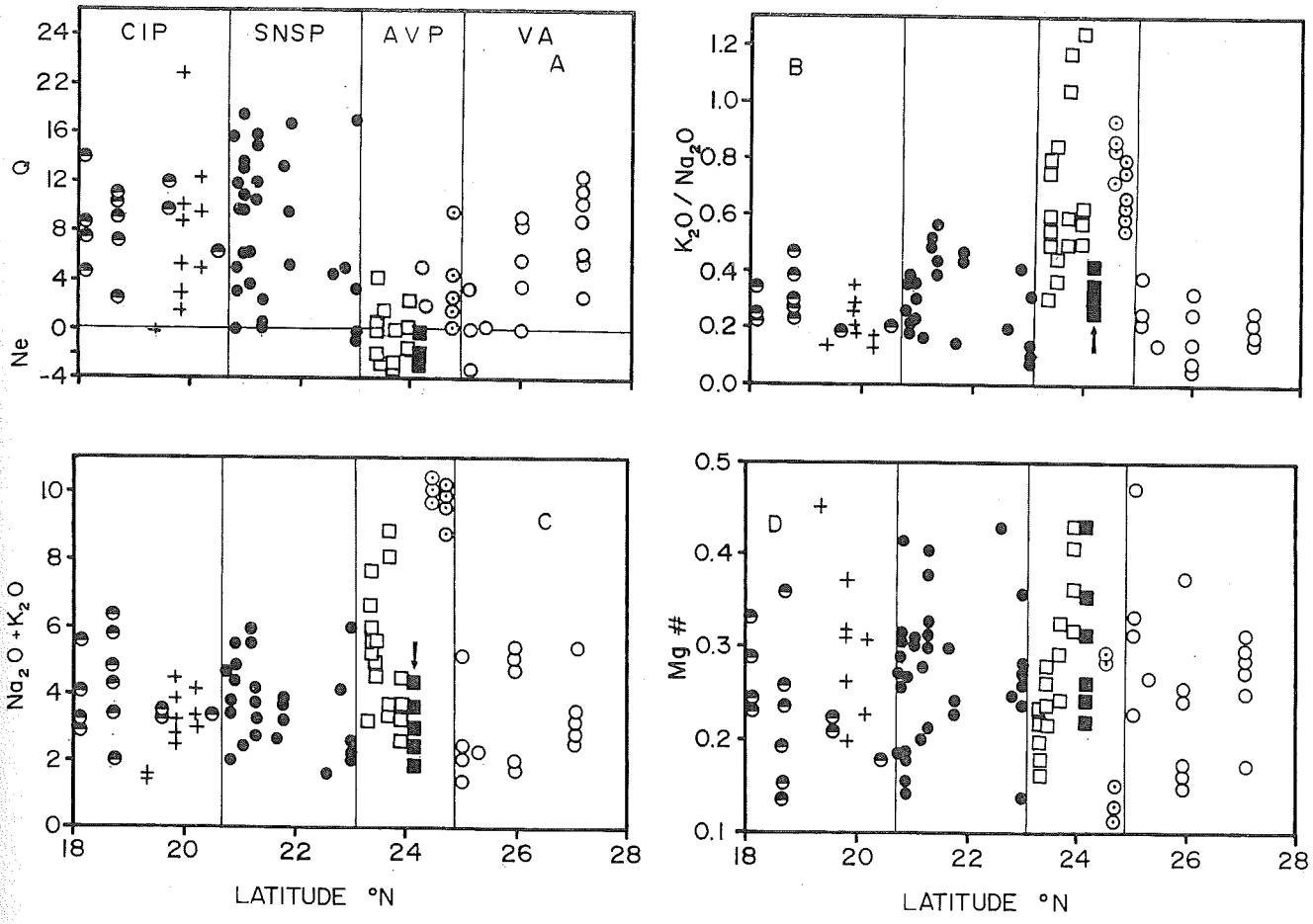


Fig. 3. Chemical variations in Mariana and Volcano arc submarine lavas versus latitude. CIP indicates the Central Island Province, SNSP the southern Northern Seamount Province, AVP the Alkalic Volcanic Province as defined in the text, and VA the northern Volcano Arc. Symbols are as in Figure 2. (a) Percent normative quartz is plotted as a positive number, percent normative nebpheline as a negative number. Arrow indicates Minami Iwo Jima, the only subalkalic volcano in the AVP; it is also extinct. On these and subsequent figures, only representative data are plotted, for clarity, as some samples have near coincident values.

(CPX:PLAG commonly 1:2, 1:3), and in some of the lavas between Nikko and Minami Iwo Jima is as abundant as PLAG. CPX usually forms subhedral to euhedral phenocrysts, and commonly occurs in glomerocrysts of five to 20 grains with titanomagnetite and plagioclase. Some of the larger CPX in the Hiyoshi Seamount lavas are optically zoned.

Phenocrysts and microphenocrysts of titanomagnetite are ubiquitous in the more siliceous samples. Amphibole is rare in the lavas of the northern CIP and NSP. It is abundant only in dacites from Cheref and Chamorro Seamounts and occurs in trace amounts in Makhanas Seamount in the CIP and Central Hiyoshi Seamount in the NSP. Biotite is found as euhedral phenocrysts in several of the more siliceous (55.6% $SiO_2$) samples from North Hiyoshi Seamount in the northern NSP (Table 2).

*Bulk Rock Chemistry*

The lavas of the northern CIP, NSP, and Volcano Arc can be divided into two groups based on their bulk chemical compositions (Figure 2). An alkalic group [*Irvine and Baragar*, 1971], characterized by high K/Na, occurs only in the northern NSP (north of Nikko) and the southern Volcano Arc from Minami Iwo Jima to Iwo Jima (Figure 2). Most of the CIP, the rest of the NSP, and the northern Volcano Arc lavas belong to a subalkalic group, with both intermediate- and low-$K_2O$ suites (Figure 2). Volcano size and K content do not seem well correlated: lavas from the large island of Agrigan belong to a medium-K series, while the large island of Nishino-shima has low-K lavas. There are seamounts with both intermediate (Kaitoku, South Daikoku) and low- (Supply Reef, Chamorro) K samples (Figure 2).

The lavas within the alkali-enriched province are distinctly less-silica saturated than lavas in the CIP, southern NSP, or the Volcano Arc (Figure 3). They commonly have high $K_2O/Na_2O$ (Figure 3) and are also enriched in Ba, Sr, $P_2O_5$, and Rb relative to the other submarine lavas (Figures 3, 4, Table 2). They include a few samples enriched in Zr (Figure 4), but in most samples in this province the alkali and alkaline-earth elements are enriched, relative to Ti, Y, and Zr. $TiO_2$ has a similar range throughout the arc (0.5-1.1%), as does Y (Figure 4). The rocks of this alkalic province also have high La/Yb and Ba/Yb [*Lin et al.*, this issue]. In the subsequent discussion we will refer to the region in which these alkali-rich samples occur as the Alkalic Volcanic Province (AVP). This includes the northern NSP (north of Nikko) and the southern Volcano Arc, from Minami Iwo Jima to Iwo Jima.

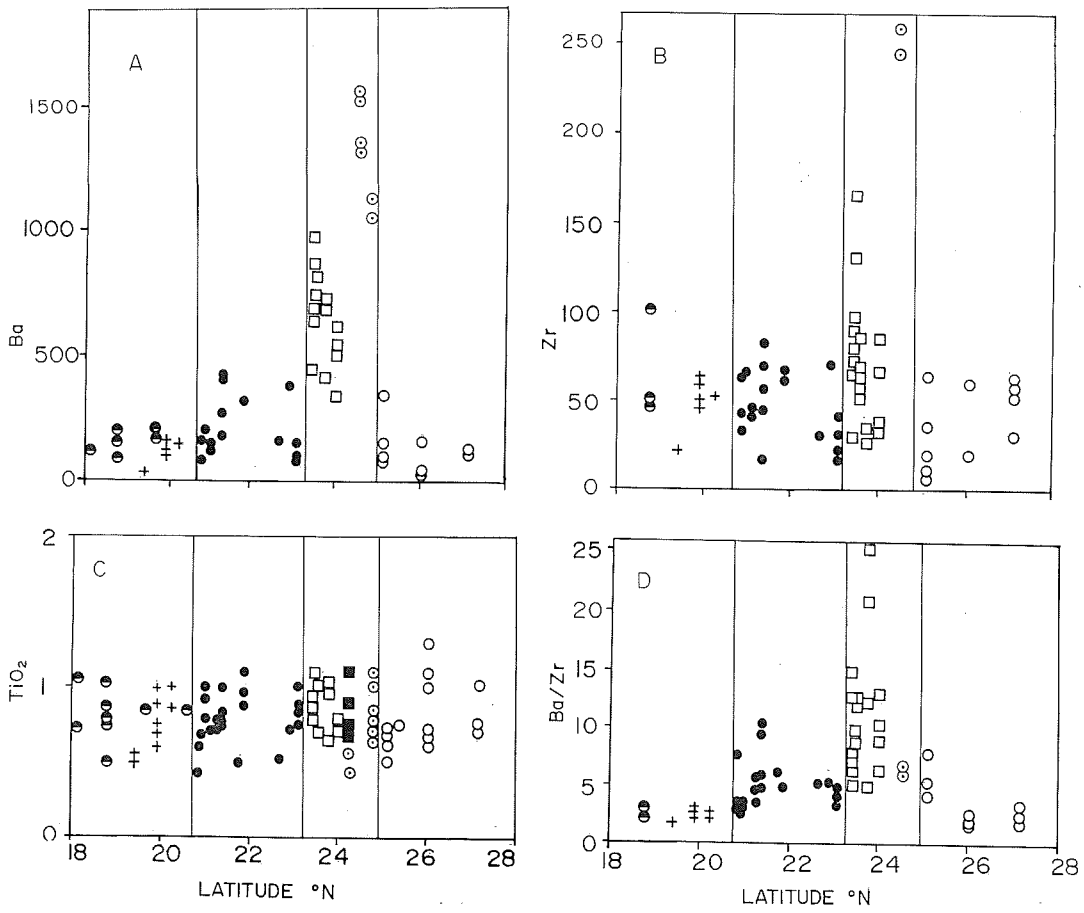


Fig. 4. Chemical variations versus latitude. Symbols and abbreviations as in Figures 2 and 3. Plots A and B include only samples with $SiO_2$ less than 55 wt. percent.

There is no apparent correlation of these enrichments with either $SiO_2$ or $Mg/Fe^{+2}+Mg$ (Mg#). Within individual edifices, the range in $SiO_2$ and Mg# is large (Figure 3). Nonetheless, both minimum and maximum values of Ba, Sr, Ba/Zr, and K/Zr are higher in the AVP than in other parts of the arc (Figure 4, Table 2).

The enrichment pattern in the AVP seems to show a distinct asymmetry. The high values of Ba, Sr, and Ba/Zr characteristic of the AVP decrease very rapidly in the Volcano Arc north of Iwo Jima (Figure 4), but there are scattered high values throughout the southern NSP. The pattern suggests an enrichment which decays more slowly to the south than to the north.

Lavas from islands in the CIP define both slightly iron-enriched trends (Agrigan [*Stern*, 1979]) and flat trends (Sarigan [*Meijer and Reagan*, 1981]) in AFM plots (Figure 5). Most of the submarine edifices in the CIP, southern NSP, and northern Volcano Arc fall within the same range in an AFM diagram as the CIP subaerial volcanos, showing slight (Kita Iwo Jima) to moderate (Kaitoku, Nikko, Eifuku) iron enrichment. Within the AVP, only Minami Iwo Jima shows a distinct iron enrichment; most of the other volcanos plot near the lower part of the CIP field (Figure 5). Iwo Jima, North Hiyoshi Seamount, and Minami Iwo Jima include compositions that are much more alkali rich than those in the rest of the arc (Figure 5).

The interelement variations of samples within and between edifices suggest that crystal-liquid fractionation may be an important control in the variation of lava composition within the arc. Ni, Cr, Sc, and CaO decrease as MgO decreases, while $SiO_2$, Zr, $Na_2O$, $K_2O$, Ba, and Rb normally increase as MgO decreases (Figure 6). V and FeO are constant, then decrease with decreasing MgO. Sr shows no consistent pattern but tends to be constant with MgO within a single edifice. The element variations are consistent with extraction of mixtures of olivine, pyroxene, and plagioclase. There is a great deal of scatter in these plots, as few of these samples are likley to lie on a liquid line of descent because of phenocryst accumulation.

*Mineral Compositions*

Variations in phenocryst compositions in lavas from the Mariana-Volcano Arc reflect the variations in bulk rock chemical compositions along the arc. Phenocrysts are commonly zoned and there are diverse compositional populations of phenocrysts within single samples.

Olivines are generally $Fo_{65}$ to $Fo_{84}$ though grains to $Fo_{87}$ and $Fo_{44}$ are found (Figure 7). Olivines are unzoned, or zoned 2-4% in Fo to more Fe-rich rims, with CaO contents of 0.3-0.5%. In rare cases (D18, Table 3), zoning may be up to 19 mol % Fo. Olivines are most iron-rich in the northern NSP. The range within single volcanos may be as great as $Fo_{42}$ to $Fo_{72}$ and within single samples up to 15 mol % Fo (Figure 7).

Plagioclases have compositions from $An_{43}$ to $An_{92}$ and have a similar range in the AVP, CIP, and southern NSP (Figure 7). Core to rim zonation can be to either more and less calcic

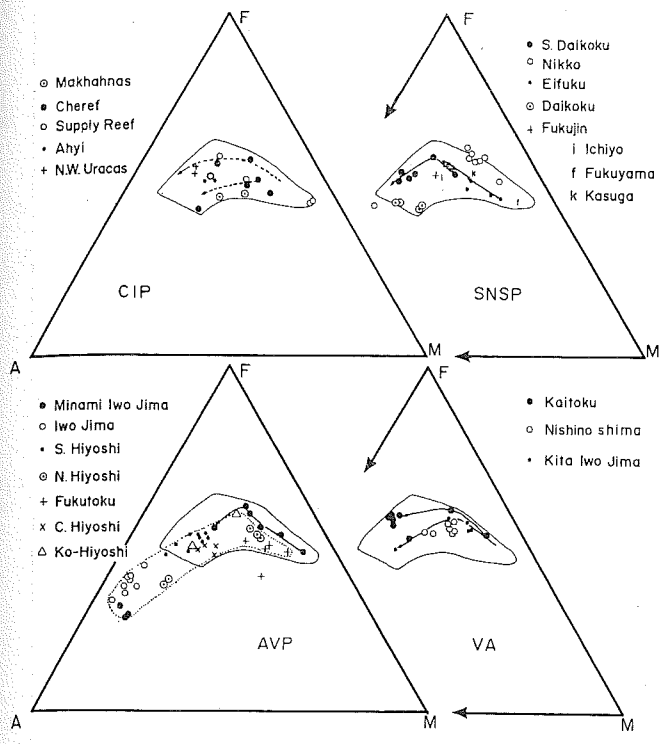


Fig. 5. AFM diagrams for lavas of the Mariana-Volcano Arc. Abbreviations for volcanic provinces as in Figure 3. The solid line encloses the field for all CIP island lavas. The upper dashed line in the CIP plot is the trend for Agrigan [*Stern*, 1979] and the lower dashed line is the trend for South Pagan [*Dixon and Batiza*, 1979]. The solid arrows in SNSP, AVP, and VA plots connect samples from single seamounts. The dotted field in the AVP plot encloses all lavas in the AVP except those of Minami Iwo Jima.

compositions. Plagioclase are commonly zoned, with variations as great as $An_{20}$ from core to rim. Compositions within single samples vary greatly, up to 20 mol % An, and ranges of 10 mol % are common (Figure 7, Table 3). PLAG in the AVP, particularly in the range $An_{30}$ to $An_{80}$, are significantly more potassic than those in the CIP and southern NSP (Figure 8).

Both CPX and OPX occur in the arc lavas. OPX range from $En_{69}Wo_2Fs_{29}$ to $En_{58}Wo_2Fs_{40}$. All are primary OPX; rare pigeonitic pyroxene occurs only in one Hiyoshi Seamount (Figure 7). CPX range in composition from $En_{50}Wo_{45}Fs_5$ to $En_{40}Wo_{42}Fs_{18}$ and, like PLAG, have diverse compositions within single samples (Figure 7). The large CPX in the Hiyoshi lavas are zoned from Mg# 0.76 to 0.37; variations from core to rim of 0.01-0.05 Mg#, and variations of 0.08 to 0.18 Mg# in CPX within single samples are not uncommon. The more ferrous CPX tend to be more sodic in the AVP than in the rest of the arc (Figure 8) but have similar $Al_2O_3$ (1-6 wt %) and $TiO_2$ (0.1-0.9 wt %). Both Ti and Al contents increase with decreasing Mg# to Mg# = 0.78; there is no consistent trend in either element at lower Mg# (Table 3).

Opaques are titanomagnetites with 5-12% $TiO_2$. Ilmenite occurs only in a gabbroic xenolith in D19. Amphiboles are relatively ferrous (Mg# = 0.62-0.73) and are calcic hornblendes (Table 3). Biotites occur in North Hiyoshi Seamount (D53, Mg# = 0.71) as phenocrysts and also are found as a mafic phase in a dioritic xenolith in D15 in the CIP (biotite Mg# = 0.58). Both amphibole and biotite occur only in the more siliceous lavas in the edifices where they are found; there is no evidence of breakdown of earlier formed biotite or amphibole in other lavas.

The changes in coexisting mineral compositions indicate crystallization from progressively more fractionated lavas. Most of the lavas in the arc are PL-OL-CPX phyric. Olivine is found as euhedral phenocrysts in lavas with up to 53% $SiO_2$ and 5% MgO, and as xenocrysts in rocks with 59% $SiO_2$ and 3% MgO. Orthopyroxene first appears in rocks with about 52% $SiO_2$ and 6% MgO and persists in most of the more siliceous and less magnesian lavas of the CIP, southern NSP, and Volcano Arc. In the AVP, OL+CPX+PLAG dominate the phenocryst assemblages, with OL < 2%. OPX is very rare, and amphibole and biotite occur in the most fractionated lavas. In the most magnesian samples in both provinces, PLAG occurs in amounts greater than or, less commonly, equal to CPX, which is more common than OL and OPX. Even the most magnesian lavas reaching the surface appear to be multiply saturated in CPX, PLAG, and OL. With increasing fractionation OL is replaced by OPX; titanomagnetite appears in most of the andesitic, and more siliceous lavas. Amphibole and biotite occur in the most fractionated lavas in the AVP.

## Discussion

The occurrence of a province of alkalic volcanism in an intraoceanic arc is of interest for several reasons. These alkalic rocks can help constrain models for temporal and spatial variation in arc volcanism and, in particular, the characteristics of arc volcanism after an episode of backarc rifting. The extreme enrichments in alkali and alkaline-earth elements in this province also provide an opportunity to identify the sources of incompatible-element enrichments in island arcs. Understanding the significance of the submarine volcanic rocks first requires identifying to what degree crystallization, melting, and source heterogeneities are responsible for their distinctive chemistry. We can then turn to a discussion of the link between tectonic setting and lava composition.

### *Intra-edifice variability*

There is considerable evidence that crystal-liquid fractionation has played a major role in the diversification of melts in the Mariana-Volcano Arc. First, there are the abundant phenocrysts themselves; none have compositions expected for mantle materials and hence reflect crystallization from silicate melts. The trends of decreasing Sc, Ni, and Cr, relatively constant Sr, and increasing large-ion lithophile (LIL) contents with decreasing MgO (Figure 6) are consistent with the evolution of liquids by extraction of PLAG, CPX, and OL.

Simplified mixing models are presented in Table 4 for representative combinations of crystal fractionation and phenocryst accumulation. We are faced with two problems in this type of modeling of crystal fractionation. First, few if any of the arc samples represent liquid compositions. The rocks are densely phyric and likely represent mixtures of liquids, phenocrysts, and xenocrysts. Second, the phenocrysts often are neither homogeneous nor in equilibrium with their host. Zoned crystals of diverse compositions are the rule rather than the exception, within individual samples. As a consequence, any single-stage fractionation or crystal accumulation model we assume for these rocks will be a gross simplification. None of the modeled pairs are likely as simple as the modeling assumes, i.e., a true liquid composition modified solely by crystal removal

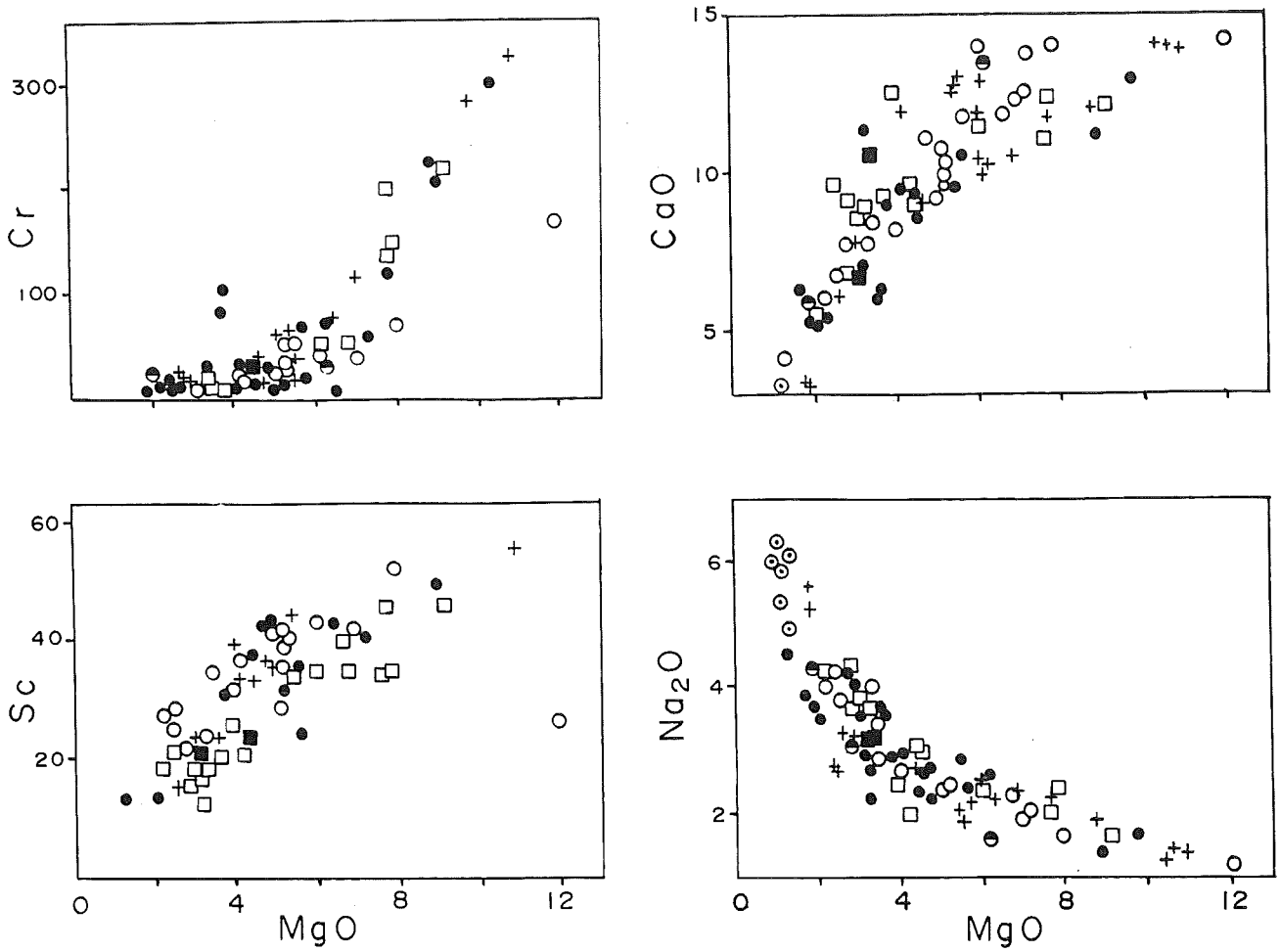


Fig. 6. Variation diagrams for Mariana and Volcano Arc lavas. Symbols as in Figure 2. Elements are in ppm and oxides in weight percent. $CaO/Al_2O_3$ also decreases sharply with decreasing MgO.

or accumulation. Each no doubt has evolved by combinations of accumulation and fractionation; those pairs that give reasonable solutions to a simple model have probably been dominated by one process or the other.

The models were constructed using analyses from Table 2 and representative mineral compositons from Table 3. The mixing problem was set up with extreme compositions of solid solution series minerals; the program was allowed to mix these as required. Calculations were done using a nonnegative least squares algorithm. Observed phenocryst assemblages and ratios of $K_2O$ contents in parent-daughter pairs were used to select physically reasonable solutions.

Most of the major element variation within edifices can be modeled by fractionation or accumulation of PLAG, OL, and CPX, with lesser amounts of OPX and magnetite (Table 4). Ten to fifty percent crystallization produces changes from basalts to basaltic andesites or andesites while variations of 10-20% in $SiO_2$ (basalt to andesite or dacite) require 70-85% crystallization. The crystallizing assemblage in both alkalic and subalkalic samples is dominated by PLAG and CPX. Ratios of CPX:PLAG vary from 0.1 to 0.7 and are not significantly different between the alkalic and subalkalic provinces. None of the AVP samples require OPX in their solutions. Crystal accumulation solutions are generally dominated by PLAG. In both fractionation and accumulation, calculated mineral proportions usually match observed modal phenocryst proportions well, after correcting for vesicularity of the samples.

Trace element models are more seriously affected by the assumption of single-stage fractionation or accumulation. While major element modeling, being simply a mass balance problem, is little affected by multiple stages of differentiation, even moderate amounts of mixing and fractionation produce marked deviations of trace element concentrations from liquid lines of descent. At best, the simple models presented here will match trace element patterns in the evolved rocks, rather than absolute abundances. In a pair dominated by crystal fractionation, the incompatible elements (Rb, Ba, K, Zr) should increase, slightly compatible elements (Sr in PLAG, Y in CPX) should increase more slowly or decrease, and the compatible elements (Ni, Cr, V) should decrease. In crystal accumulation, the incompatible elements will be diluted and the compatible elments will be constant or slightly higher or lower depending on the phase being accumulated.

If we model the calculated fractionation schemes (Table 4) by simple Rayleigh fractionation and the crystal accumulation by mass balance, the models do, in most cases, produce the right kinds of variations: fractionation raises Rb, K, Ba, and Sr, decreases Sc and Y slightly, and greatly decreases Sc, V, and Cr (Figure 9). Dilution by crystal accumulation has the opposite effects (Figure 9). The fits are best for small degrees of

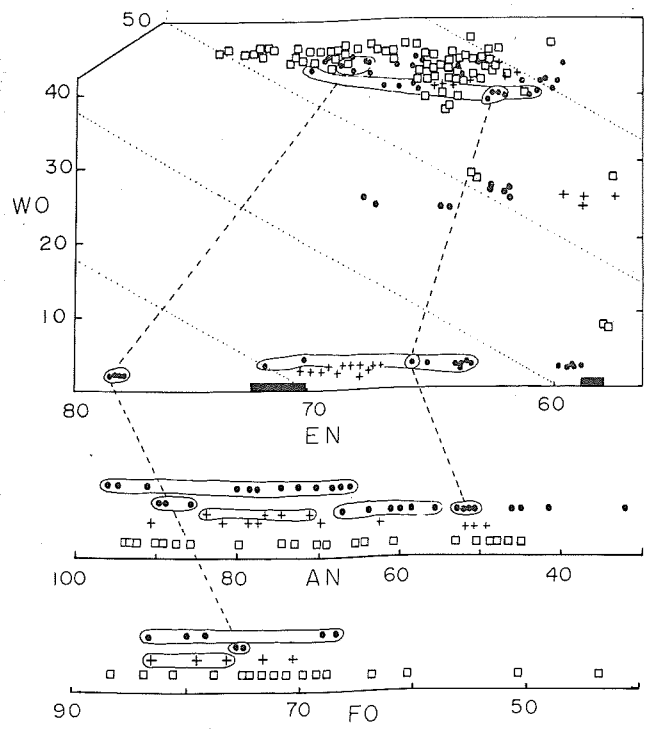


Fig. 7. Representative mineral compositions for Mariana-Volcano Arc lavas. Symbols as in Figure 2. The upper portion of the diagram is a portion of the pyroxene quadrilateral. Dotted lines are lines of constant En. Lower plots show ranges of compositions for representative PLAG and OL from each volcanic province. Solid lines enclose compositions found within single samples. Dashed lines connect coexisting mineral compositions in samples whose minerals have a relatively limited compositional range. Points plotting between $Wo_{25}$ and $Wo_{30}$ are amphibole anlayses. Solid bars on base of quadrilateral indicate range of Mg# in biotites from North Hiyoshi (Mg# = 0.70-0.72) and from a dioritic xenolith in D15.

fractionation or accumulation. At large F the calculated compositions diverge from measured values, particularly for the LIL, perhaps indicating open system crystallization (Figure 9, model 15). Cr variations are not well fit in many models because of the low abundance of Cr in many samples ($10 \pm 6$ ppm).

Though fractionation or crystal accumulation can account for the variation between many of the samples, some of the major element models are clearly not satisfactory, despite giving mathematically reasonable solutions (Table 4). Calculated trace element concentrations for some pairs from Ahyi (Figure 9, model 6) and Nikko (model 14) are too dilute or concentrated and, in the former case, do not fit the trace element pattern at all. These pairs often give solutions requiring unreasonable degrees of crystal separation or unrealistic mineral proportions, based on modal assemblages. These pairs may represent rocks related by multiple episodes of fractionation and accumulation or rocks derived from distinct batches of magma.

The calculations do indicate that with sufficiently detailed petrographic and mineralogic data, much of the variation within each of these centers can be modeled by crystal accumulation and crystal-liquid fractionation. The commmon occurrence of normally and reversely zoned crystals, resorbed crystals, and diverse phenocryst compositions in single samples indicates that the fractionation is dominated by open-system processes.

The conditions of crystallization are somewhat difficult to constrain. The common occurrence of disequilibrium phenocryst assemblages precludes any meaningful calculations of temperatures from pyroxene pairs or olivine-glass pairs, at least from the reconnaissance probe studies presented here. The most magnesian and aphyric samples in both subalkalic and alkalic groups are multiply saturated in OL-CPX-PLAG. The OL is > $Fo_{80}$, the PLAG > $An_{85}$, and the CPX has Mg# > 0.84 and $Al_2O_3 < 2\%$.

Experiments on high-Al, magnesian basalts show a shrinking of the olivine phase volume with pressure, so that at low P the

TABLE 3a. Representative Mineral Analyses of Phenocrysts in Lavas From Submarine Volcanos in the Northern Mariana and SouthernVolcano Arc: Amphiboles and Biotites

| | Ahyi | | Makhahnas | Chamorro | C. Hiyoshi | Ahyi | N. Hiyoshi |
|---|---|---|---|---|---|---|---|
| | D15-2-2 | D15-M2 | D18-7 | D23-3 | D52-3-1 | D15-M2 | D53-1-2 |
| Type | gs | r | | | | | |
| $SiO_2$ | 48.87 | 49.72 | 45.27 | 49.32 | 41.39 | 37.96 | 38.35 |
| $TiO_2$ | 0.31 | 1.08 | 2.01 | 1.15 | 2.49 | 3.98 | 5.03 |
| $Al_2O_3$ | 7.54 | 5.55 | 9.81 | 7.06 | 13.06 | 13.28 | 14.28 |
| FeO | 8.87 | 15.79 | 12.8 | 12.98 | 11.9 | 17.64 | 12.67 |
| MnO | 0.61 | 0.34 | 0.49 | 0.7 | 0.23 | 0.19 | 0.19 |
| MgO | 13.51 | 14.4 | 14.74 | 16.07 | 14.42 | 13.99 | 16.75 |
| CaO | 19.06 | 10.7 | 11.25 | 10.62 | 11.71 | 0.05 | 0.11 |
| $Na_2O$ | 0.42 | 1.15 | 1.81 | 1.25 | 2.32 | 0.22 | 0.67 |
| $K_2O$ | 0.06 | 0.21 | 0.31 | 0.16 | 0.87 | 8.52 | 8.47 |
| SUM | 99.25 | 98.94 | 98.5 | 99.31 | 98.39 | 95.83 | 96.53 |
| Mg# | 0.732 | 0.620 | 0.674 | 0.689 | 0.685 | 0.587 | 0.703 |

Analyses used a general silicate standardization which produces slightly high sums for magnesian olivines and orthopyroxenes. Types are r, rim analysis; c, core analysis; s, analysis of a small grain; g, analysis of a groundmass mineral; x, an analysis of a xenocryst; and m an analysis of a medium-grained crystal. Analyses not marked by a g are of phenocrysts.

TABLE 3b. Representative Mineral Analyses of Phenocrysts in Lavas From Submarine Volcanos in the Northern Mariana and Southern Volcano Arc: Spinels

| | Ahyi | NW Uracas | Nikko | C. Hiyoshi | Fukutoku |
|---|---|---|---|---|---|
| | D15-2-2 | D19-3-3 | D45-11 | D52-3-2 | D55-1-2 |
| Type | g | r | c | | |
| $SiO_2$ | 0.25 | 0.41 | 0.23 | 0.21 | 0.23 |
| $TiO_2$ | 9.27 | 33.48 | 12.21 | 8.96 | 8.03 |
| $Al_2O_3$ | 6.46 | 7.4 | 3.83 | 5.37 | 7.46 |
| FeO | 79.52 | 55.25 | 78.4 | 79.75 | 77.44 |
| MnO | 0.46 | 0.46 | 0.74 | 0.69 | 0.5 |
| MgO | 2.61 | 2.05 | 2.61 | 2.33 | 3.9 |
| CaO | 0.17 | 0.23 | 0.14 | 0.14 | 0.13 |
| $Na_2O$ | 0.03 | 0.09 | 0.01 | 0.01 | 0.02 |
| $K_2O$ | 0.07 | 0.05 | 0.05 | 0.05 | 0.06 |
| SUM | 98.82 | 99.42 | 98.24 | 97.49 | 97.76 |

Analyses used a general silicate standardization which produces slightly high sums for magnesian olivines and orthopyroxenes. Types are r, rim analysis; c, core analysis; s, analysis of a small grain; g, analysis of a groundmass mineral; x, an analysis of a xenocryst; and m an analysis of a medium-grained crystal. Analyses not marked by a g are of phenocrysts .

crystallization sequence is OL-PLAG-CPX, at 5-10 kbar it is OL-CPX-PLAG, and over 10 kbar it is CPX-OPX-PLAG [*Gust and Perfit*, 1987]. In shoshonitic lavas (6% MgO, 0.82% $K_2O$) pressure has a similar effect [*Meen*, 1987]. At 1 atm the crystallization sequence is PLAG-OL-CPX, while at 10 kbar it is PL-OPX-CPX. There is no evidence for an early crystallization of OPX in the Mariana-Volcano Arc lavas. OPX occurs in most of the Mariana-Volcano Arc samples at relatively low Mg# (0.72-0.78) and appears to be crystallizing well after OL, CPX, and PLAG. The magnesian CPX in the arc samples have low $Al_2O_3$ (< 2%), whereas CPX crystallized at 10 kbar tend to be aluminous [*Gust and Perfit*, 1987]. The relatively magnesian compositions of coexisting CPX and OL in the Mariana-Volcano Arc lavas suggest that neither crystallized alone, or with PLAG, for any significant temperature interval before joined by the other phase; the pressure of crystallization must have been high enough that CPX and OL appeared close together. In general, the anhydrous phase equilibria studies are consistent with the crystallization of most of the Mariana-Volcano arc lavas at 5 kbar or less.

$H_2O$ will expand the primary volume of olivine [*Kushiro*, 1969] and will raise the pressure at which the OL-PLAG-CPX will be the liquidus sequence. The volatile contents of these melts has not been measured, but analyses of other Mariana Arc basalts [*Dixon and Batiza*, 1979] suggest volatile contents of 1-3% are likely. If this is primarily $H_2O$, the crystallization could be at significantly higher pressure, though such crystallization would still be expected to produce more aluminous pyroxenes than are observed.

### *Inter-edifice Variations*

The most striking feature of the Mariana-Volcano Arc lavas is the existence of the potassic volcanic province in the northern Mariana Arc and the southern Volcano Arc. If much of the variation within individual centers can be explained by crystal fractionation and accumulation from magnesian lavas, we are left with the question of the origin of the differences between the volcanic centers. The most magnesian basalts from the submarine edifices have MgO > 8%, Cr > 100 ppm, and high

TABLE 3c. Representative Mineral Analyses of Phenocrysts in Lavas From Submarine Volcanos in the Northern Mariana and Southern Volcano Arc: Orthopyroxenes

| | Ahyi | Makhahnas | | Daikoku | | Kasuga | | Nikko | C. Hiyoshi |
|---|---|---|---|---|---|---|---|---|---|
| | D15-2-2 | D18-7 | D18-7 | D29-1-1 | D29-1-1 | D33-1-1 | D33-1-1 | D45-11 | D52-3-2 |
| Type | g | g | g | g | g | | c | s | gr |
| $SiO_2$ | 53.48 | 53.62 | 51.24 | 51.63 | 52.67 | 53.98 | 52.46 | 54.28 | 52.32 |
| $TiO_2$ | 0.25 | 0.22 | 0.23 | 0.36 | 0.32 | 0.21 | 0.23 | 0.28 | 0.29 |
| $Al_2O_3$ | 1.17 | 1.28 | 5.63 | 1.93 | 3.6 | 1.41 | 0.79 | 1.19 | 0.58 |
| FeO | 20.5 | 19.95 | 18.13 | 22.3 | 17.69 | 22.52 | 25.11 | 20.78 | 23.43 |
| MnO | 0.81 | 1.03 | 0.84 | 0.84 | 0.44 | 0.65 | 0.89 | 0.88 | 1.34 |
| MgO | 23.86 | 23.71 | 23.63 | 22.3 | 26.04 | 22.62 | 20.88 | 22.87 | 18.78 |
| CaO | 1.5 | 1.29 | 1.25 | 1.93 | 1.91 | 1.41 | 1.5 | 1.78 | 4.01 |
| $Na_2O$ | 0.06 | 0.03 | 0.04 | 0.05 | 0.03 | 0.04 | 0.06 | 0.05 | 0.08 |
| $K_2O$ | 0.02 | 0.03 | 0.01 | 0.04 | 0.02 | 0.03 | 0.03 | 0 | 0.02 |
| SUM | 101.66 | 101.15 | 101.01 | 101.38 | 102.72 | 102.87 | 101.94 | 102.10 | 100.85 |
| Mg# | 0.676 | 0.680 | 0.700 | 0.642 | 0.725 | 0.643 | 0.598 | 0.664 | 0.590 |

Analyses used a general silicate standardization which produces slightly high sums for magnesian olivines and orthopyroxenes. Types are r, rim analysis; c, core analysis; s, analysis of a small grain; g, analysis of a groundmass mineral; x, an analysis of a xenocryst; and m an analysis of a medium-grained crystal. Analyses not marked by a g are of phenocrysts

TABLE 3d. Representative Mineral Analyses of Phenocrysts in Lavas From Submarine Volcanos in the Northern Mariana and Southern Volcano Arc: Olivines

| | Ahyi | Makhahnas | Eifuku | Nikko | | | | | | Ko-Hiyoshi | |
|---|---|---|---|---|---|---|---|---|---|---|---|
| | D15-2-2 | D18-7 | D31-1-4 | D45-1-2 | D45-3 | D45-3 | 46-5-1 | D46-5-1 | D46-5-1 | D47-1-8 | D47-1-8 |
| Type | s | g | gc | s | r | c | c | r | gs | c | r |
| $SiO_2$ | 39.18 | 40.36 | 38.57 | 37.95 | 38.95 | 38.87 | 40.82 | 40.64 | 38.46 | 38.84 | 38.87 |
| $TiO_2$ | 0.08 | 0.03 | 0.06 | 0.08 | 0.05 | 0.06 | 0.04 | 0.04 | 0.06 | 0.06 | 0.06 |
| $Al_2O_3$ | 0.04 | 0.01 | 0 | 1.42 | 0.03 | 0.04 | 0 | 0.05 | 0.02 | 0.37 | 0.07 |
| FeO | 27.46 | 16.39 | 26.17 | 30.28 | 24.7 | 23.91 | 15.75 | 19.18 | 29.17 | 26.78 | 28.39 |
| MnO | 0.53 | 0.29 | 0.52 | 0.69 | 0.44 | 0.43 | 0.31 | 0.35 | 0.59 | 0.64 | 0.77 |
| MgO | 36.83 | 45.11 | 37.75 | 32.72 | 37.85 | 36.73 | 45.14 | 43.55 | 35.29 | 36.06 | 34.66 |
| CaO | 0.2 | 0.2 | 0.3 | 0.33 | 0.28 | 0.31 | 0.3 | 0.31 | 0.36 | 0.25 | 0.22 |
| $Na_2O$ | 0 | 0.02 | 0.02 | 0.05 | 0.01 | 0.02 | 0.03 | 0.02 | 0.01 | 0 | 0.02 |
| $K_2O$ | 0.02 | 0.01 | 0.02 | 0.02 | 0.01 | 0.02 | 0 | 0.02 | 0.03 | 0.03 | 0.02 |
| SUM | 104.36 | 102.42 | 103.4 | 103.55 | 102.32 | 100.37 | 102.39 | 104.16 | 103.99 | 103.04 | 103.07 |
| Mg# | 0.706 | 0.831 | 0.721 | 0.659 | 0.733 | 0.734 | 0.837 | 0.803 | 0.684 | 0.707 | 0.686 |

| | Central Hiyoshi | | North Hiyoshi | | Fukutoku | | | |
|---|---|---|---|---|---|---|---|---|
| | D52-3-2 | D52-3-2 | D54-1-1 | D54-1-1 | D55-1-2 | 55-1-2 | D57-5 | D57-5 |
| Type | s | s | r | c | r | | | |
| $SiO_2$ | 35.49 | 37.68 | 39.4 | 40.53 | 38.15 | 39.67 | 42.61 | 34.71 |
| $TiO_2$ | 0.12 | 0.07 | 0.0 5 | 0.04 | 0.11 | 0.08 | 0.03 | 0.17 |
| $Al_2O_3$ | 0.05 | 0.41 | | 0 0.11 | 1.7 | 0.01 | 0.06 | 1.01 |
| FeO | 45.73 | 29.47 | 23.4 4 | 15.62 | 27.9 | 24.47 | 13.11 | 38.72 |
| MnO | 1.26 | 0.89 | 0. 5 | 0.3 | 0.69 | 0.53 | 0.25 | 0.73 |
| MgO | 19.74 | 32.55 | 39.5 8 | 44.94 | 31.69 | 38.05 | 47.32 | 21.92 |
| CaO | 0.24 | 0.22 | 0. 3 | 0.32 | 1.7 | 0.27 | 0.32 | 0.76 |
| $Na_2O$ | 0.01 | 0.01 | 0.0 3 | 0 | 0.25 | 0.02 | 0.02 | 0.11 |
| $K_2O$ | 0.05 | 0.02 | 0.0 1 | 0 | 0.09 | 0.01 | 0 | 0.05 |
| SUM | 102.68 | 101.32 | 103.3 2 | 101.87 | 102.28 | 103.11 | 103.69 | 98.17 |
| Mg# | 0.436 | 0.664 | 0.75 2 | 0.838 | 0.671 | 0.736 | 0.866 | 0.504 |

Analyses used a general silicate standardization which produces slightly high sums for magnesian olivines and orthopyroxenes. Types are r, rim analysis; c, core analysis; s, analysis of a small grain; g, analysis of a groundmass mineral; x, an analysis of a xenocryst; and m an analysis of a medium-grained crystal. Analyses not marked by a g are of phenocrysts

$CaO/Al_2O_3$ (Table 5). The most pronounced differences along the arc are between the high-K lavas of the AVP and the low-K lavas of the CIP and Volcano Arc. From the CIP to AVP magnesian lavas, $K_2O$ goes up by a factor of 5, Ba by 6, Sr by 3.5, Y by 1.5-2, Ti by 1.5, and Zr by about 2 (Table 5).

The first possible explanation for these differences is that the potassic series are derived by high-pressure crystallization of a low-K subalkaline basalt. Crystallization of PL-OPX-CPX at >8 kbar will produce a high-$K_2O$, low-$SiO_2$ enrichment trend from the same lavas that give rise to low-K, tholeiitic fractionation trends at low pressure (Figure 10, [*Meen*, 1987]). Indeed an alkalic basalt from North Hiyoshi Seamount can be derived from the low-$K_2O$ basalts by removal of about 20% PLAG, 30% CPX, 10% OPX, and 0-5% OL (Table 4). However, such an extraction is at odds with the common occurrence of OL, lack of OPX, and low-alumina CPX in the potassic magmas. The fractionation trends within each group do not track back to the same parental basalt compositions (Figure 10) and the trace element patterns of the potassic rocks are not well fit by pyroxene-dominated fractionation. In particular, such crystallization does not fractionate Ba or K from Zr as required, the extensive plagioclase fractionation greatly depletes Sr, and the pyroxene crystallization produces very low concentrations of V, Sc, Cr, and Ni in the derivative, high-K lavas (Figure 9). Neither will this fractionation produce the prominent light rare earth (LREE) enrichments characteristic of the AVP [*Lin et al.*, this issue].

The differences between the magnesian melts in the CIP and

TABLE 3e. Representative Mineral Analyses of Phenocrysts in Lavas From Submarine Volcanos in the Northern Mariana and Southern Volcano Arc: Clinopyroxene

| | Ahyi | | Makhahnas | | Daikoku | | | Eifuku | | Kasuga | |
|---|---|---|---|---|---|---|---|---|---|---|---|
| | D15-2-2 | D15-2-2 | D18-7 | D18-7 | D29-1-1 | D29-1-1 | D29-1-1 | D31-1-4 | D31-1-4 | 33-1-1 | D33-1-1 |
| Type | s | g | g | | g | r | r | gr | gc | gc | s |
| $SiO_2$ | 51.35 | 52.01 | 50.65 | 52.04 | 51.13 | 52.17 | 52.74 | 51.55 | 52.02 | 53.06 | 50.61 |
| $TiO_2$ | 0.5 | 0.43 | 0.48 | 0.49 | 0.59 | 0.45 | 0.35 | 0.52 | 0.59 | 0.33 | 0.61 |
| $Al_2O_3$ | 3.09 | 2.71 | 2.8 | 2.19 | 2.68 | 1.91 | 3.2 | 3.34 | 3.19 | 1.28 | 4.92 |
| FeO | 9.6 | 9.45 | 10.45 | 8.86 | 11.94 | 10.91 | 5.22 | 8.83 | 9.58 | 11.64 | 11.14 |
| MnO | 0.34 | 0.56 | 0.64 | 0.5 | 0.54 | 0.55 | 0.19 | 0.28 | 0.27 | 0.47 | 0.34 |
| MgO | 15.83 | 15.43 | 13.81 | 14.72 | 14.31 | 15.01 | 16.86 | 15.92 | 15.05 | 13.92 | 14.27 |
| CaO | 20.6 | 20.82 | 20.53 | 21.48 | 19.99 | 19.82 | 21.45 | 20.32 | 20.5 | 20.91 | 20.55 |
| $Na_2O$ | 0.23 | 0.35 | 0.35 | 0.32 | 0.3 | 0.28 | 0.24 | 0.25 | 0.27 | 0.26 | 0.27 |
| $K_2O$ | 0.03 | 0.03 | 0.03 | 0.02 | 0.03 | 0.04 | 0.12 | 0 | 0.01 | 0.02 | 0.02 |
| SUM | 101.56 | 101.79 | 99.75 | 100.62 | 101.5 | 101.14 | 100.37 | 101.00 | 101.47 | 101.88 | 102.72 |
| Mg# | 0.747 | 0.745 | 0.703 | 0.749 | 0.682 | 0.711 | 0.853 | 0.764 | 0.738 | 0.682 | 0.697 |

| | Nikko | | | | | North Hiyoshi | | | | | |
|---|---|---|---|---|---|---|---|---|---|---|---|
| | D45-11 | D46-5-1 | D46-5-1 | D46-5-1 | D46-5-1 | D53-1-2 | 53-1-2 | D53-1-2 | D54-1-1 | D54-1-1 | D54-1-1 |
| Type | c | g | s | r | c | r | s | c | r | | s |
| $SiO_2$ | 52.95 | 51.69 | 53.08 | 50.02 | 50.78 | 54.4 | 53.99 | 53.66 | 50.77 | 53.05 | 51.35 |
| $TiO_2$ | 0.49 | 0.64 | 0.34 | 0.72 | 0.34 | 0.31 | 0.35 | 0.26 | 0.78 | 0.26 | 0.74 |
| $Al_2O_3$ | 1.46 | 3.23 | 2.48 | 5.35 | 5.26 | 1.48 | 2.88 | 1.3 | 4.64 | 2.57 | 4.5 |
| FeO | 11.08 | 9.94 | 7.09 | 8.38 | 5.19 | 9.03 | 9.14 | 9.08 | 8.72 | 4.42 | 8.39 |
| MnO | 0.57 | 0.31 | 0.21 | 0.21 | 0.13 | 0.75 | 0.71 | 0.84 | 0.23 | 0.15 | 0.22 |
| MgO | 14.63 | 14.73 | 16.66 | 14.32 | 16.05 | 15.92 | 15.13 | 15.09 | 13.55 | 17.18 | 14.56 |
| CaO | 19.42 | 21.84 | 21.91 | 21.71 | 22.9 | 20.9 | 20.13 | 21.82 | 21.81 | 22.21 | 22.61 |
| $Na_2O$ | 0.3 | 0.3 | 0.2 | 0.24 | 0.19 | 0.36 | 0.41 | 0.46 | 0.31 | 0.23 | 0.29 |
| $K_2O$ | 0 | 0.02 | 0.02 | 0.03 | 0.03 | 0 | 0.01 | 0.02 | 0 | 0.01 | 0 |
| SUM | 100.91 | 102.69 | 101.97 | 100.91 | 100.86 | 103.16 | 102.75 | 102.52 | 100.8 | 100.09 | 102.66 |
| Mg# | 0.703 | 0.726 | 0.808 | 0.754 | 0.847 | 0.760 | 0.748 | 0.749 | 0.736 | 0.874 | 0.757 |

| | Central Hiyoshi | | Fukutoku | | | | | |
|---|---|---|---|---|---|---|---|---|
| | D52-3-2 | D52-3-2 | D55-1-2 | D55-1-2 | D55-1-2 | D57-5 | D57-5 | D57-5 |
| Type | gr | c | | | r | | r | c |
| $SiO_2$ | 53.00 | 51.06 | 53.07 | 54.32 | 51.84 | 50.96 | 52.35 | 54.86 |
| $TiO_2$ | 0.42 | 0.65 | 0.37 | 0.19 | 0.91 | 0.4 | 0.35 | 0.15 |
| $Al_2O_3$ | 1.03 | 4.11 | 3.45 | 1.5 | 5.06 | 4.11 | 3.55 | 1.21 |
| FeO | 17.42 | 7.97 | 5.11 | 2.98 | 9.17 | 6.18 | 5.68 | 2.98 |
| MnO | 0.99 | 0.28 | 0.18 | 0.13 | 0.23 | 0.2 | 0.19 | 0.14 |
| MgO | 15.21 | 14.27 | 16.19 | 18.06 | 14.46 | 15.45 | 16.19 | 17.70 |
| CaO | 13.96 | 22.06 | 22.89 | 23.35 | 21.41 | 22.49 | 22.67 | 23.78 |
| $Na_2O$ | 0.27 | 0.27 | 0.14 | 0.2 | 0.37 | 0.24 | 0.19 | 0.15 |
| $K_2O$ | 0.03 | 0.01 | 0.01 | 0 | 0 | 0 | 0.04 | 0 |
| SUM | 102.31 | 100.67 | 101.4 | 100.72 | 103.46 | 100.03 | 101.21 | 100.97 |
| Mg# | 0.610 | 0.762 | 0.850 | 0.916 | 0.739 | 0.818 | 0.836 | 0.914 |

Analyses used a general silicate standardization which produces slightly high sums for magnesian olivines and orthopyroxenes. Types are r, rim analysis; c, core analysis; s, analysis of a small grain; g, analysis of a groundmass mineral; x, an analysis of a xenocryst; and m an analysis of a medium-grained crystal. Analyses not marked by a g are of phenocrysts

TABLE 3f. Representative Mineral Analyses of Phenocrysts in Lavas From Submarine Volcanos in the Northern Mariana and Southern Volcano Arc: Plagioclase

| | Ahyi | | | | Makhahnas | | | Daikoku | | | |
|---|---|---|---|---|---|---|---|---|---|---|---|
| | D15-2-2 | D15-2-2 | D15-2-2 | D15-2-2 | D18-7 | D18-7 | D18-7 | D29-1-1 | D29-1-1 | D29-1-1 | D29-1-1 |
| Type | c | m | r | m | c | m | r | | r | g | m |
| $SiO_2$ | 44.51 | 52.37 | 49.72 | 58.51 | 47.50 | 52.63 | 52.18 | 45.75 | 54.18 | 53.01 | 54.92 |
| $TiO_2$ | 0.03 | 0.06 | 0.04 | 0.32 | 0.04 | 0.04 | 0.05 | 0.04 | 0.05 | 0.05 | 0.06 |
| $Al_2O_3$ | 36.53 | 30.52 | 32.92 | 24.15 | 33.25 | 29.78 | 30.18 | 35.56 | 28.9 | 30.26 | 29.57 |
| FeO | 0.63 | 0.82 | 0.65 | 3.16 | 0.64 | 0.61 | 0.55 | 0.85 | 0.7 | 0.71 | 0.74 |
| MnO | 0.04 | 0.04 | 0.04 | 0.08 | 0.02 | 0.05 | 0.02 | 0.03 | 0.02 | 0.01 | 0.03 |
| MgO | 0.06 | 0.13 | 0.07 | 0.99 | 0.03 | 0.06 | 0.07 | 0.1 | 0.15 | 0.08 | 0.14 |
| CaO | 18.37 | 13.54 | 15.42 | 8.81 | 16.92 | 13.2 | 13.26 | 18.87 | 11.27 | 13.05 | 11.41 |
| $Na_2O$ | 1.04 | 3.66 | 2.81 | 4.56 | 1.78 | 3.85 | 4.05 | 0.81 | 4.9 | 4.04 | 4.8 |
| $K_2O$ | 0.03 | 0.09 | 0.05 | 0.48 | 0.05 | 0.13 | 0.1 | 0.04 | 0.24 | 0.17 | 0.25 |
| SUM | 101.24 | 101.23 | 101.73 | 101.04 | 100.22 | 100.35 | 100.46 | 102.05 | 100.40 | 101.37 | 101.94 |
| AN | 0.906 | 0.670 | 0.751 | 0.515 | 0.839 | 0.653 | 0.642 | 0.927 | 0.558 | 0.639 | 0.566 |

| | Eifuku | | | | Kasuga | | | Nikko | | | |
|---|---|---|---|---|---|---|---|---|---|---|---|
| | D31-1-4 | D31-1-4 | D31-1-4 | D33-1-1 | D33-1-1 | D33-1-1 | D33-1-1 | D45-3 | D45-3 | D45-3 | D45-3 |
| Type | m | r | c | r | c | r | s | r | c | r | s |
| $SiO_2$ | 49.72 | 48.29 | 47.86 | 50.95 | 45.74 | 46.48 | 49.54 | 48.47 | 47.36 | 48.94 | 50.44 |
| $TiO_2$ | 0.06 | 0.04 | 0.06 | 0.03 | 0.04 | 0.03 | 0.03 | 0.04 | 0.04 | 0.04 | 0.04 |
| $Al_2O_3$ | 32.15 | 33.87 | 33.53 | 31.78 | 36.71 | 34.73 | 31.53 | 34.15 | 34.34 | 33.3 | 32.27 |
| FeO | 0.94 | 0.83 | 0.81 | 0.52 | 0.5 | 0.61 | 0.63 | 0.87 | 0.79 | 0.9 | 0.95 |
| MnO | 0.04 | 0.02 | 0.04 | 0.03 | 0.03 | 0.05 | 0.01 | 0.04 | 0.05 | 0.03 | 0.02 |
| MgO | 0.13 | 0.16 | 0.14 | 0.05 | 0.12 | 0.13 | 0.11 | 0.16 | 0.1 | 0.22 | 0.16 |
| CaO | 15.57 | 16.44 | 16.92 | 15 | 19.9 | 18.79 | 15.61 | 17.57 | 17.75 | 15.82 | 14.85 |
| $Na_2O$ | 2.41 | 2.0 | 1.9 | 3.09 | 0.43 | 1.0 | 2.62 | 1.53 | 1.27 | 2.29 | 3.04 |
| $K_2O$ | 0.13 | 0.09 | 0.07 | 0.05 | 0.03 | 0.03 | 0.04 | 0.04 | 0.02 | 0.05 | 0.04 |
| SUM | 101.14 | 101.73 | 101.33 | 101.49 | 103.5 | 101.84 | 100.11 | 102.86 | 101.70 | 101.58 | 101.81 |
| AN | 0.780 | 0.819 | 0.830 | 0.727 | 0.962 | 0.912 | 0.766 | 0.863 | 0.885 | 0.791 | 0.728 |

| | Nikko | | | | Central Hiyoshi | | | | |
|---|---|---|---|---|---|---|---|---|---|
| | D45-11 | D45-11 | D46-5-1 | D46-5-1 | D52-3-2 | D52-3-2 | D52-3- 2 | D52-3-2 | D52-3-2 |
| Type | c | r | r | c | s | c | r | c | r |
| $SiO_2$ | 56.39 | 56.2 | 48.00 | 46.00 | 55.63 | 50.02 | 59.98 | 47.50 | 49.00 |
| $TiO_2$ | 0.06 | 0.06 | 0.05 | 0.02 | 0.07 | 0.05 | 0.07 | 0.04 | 0.04 |
| $Al_2O_3$ | 28.42 | 28.63 | 33.87 | 35.35 | 28.56 | 32.43 | 25.53 | 34.13 | 32.59 |
| FeO | 0.6 | 0.69 | 0.85 | 0.69 | 0.76 | 0.6 | 0.65 | 0.64 | 0.74 |
| MnO | 0.02 | 0.06 | 0.05 | 0.02 | 0.01 | 0.04 | 0 | 0.04 | 0.04 |
| MgO | 0.08 | 0.09 | 0.23 | 0.11 | 0.03 | 0.07 | 0.05 | 0.07 | 0.04 |
| CaO | 10.63 | 11.36 | 17.69 | 18.69 | 10.77 | 15.48 | 7.33 | 17.56 | 15.69 |
| $Na_2O$ | 5.24 | 4.89 | 1.6 | 0.89 | 5.12 | 2.64 | 6.85 | 1.39 | 2.36 |
| $K_2O$ | 0.12 | 0.11 | 0.03 | 0.03 | 0.34 | 0.18 | 0.8 | 0.06 | 0.13 |
| SUM | 101.57 | 102.08 | 102.37 | 101.79 | 101.29 | 101.50 | 101.26 | 101.43 | 100.62 |
| AN | 0.527 | 0.560 | 0.858 | 0.920 | 0.536 | 0.763 | 0.370 | 0.874 | 0.785 |

TABLE 3f. (continued)

| | North Hiyoshi | | | | | | Fukutoku | | | | |
|---|---|---|---|---|---|---|---|---|---|---|---|
| | D53-1-2 | D53-1-2 | D53-1-2 | D53-1-2 | D54-1-1 | D54-1-1 | D55-1-2 | D55-1-2 | D55-1-2 | D55-1-2 | D55-1-2 |
| Type | x | c | r | c | s | c | r | r | c | s | s |
| $SiO_2$ | 46.25 | 47.57 | 57.63 | 56.82 | 47.91 | 48.01 | 48.24 | 51.46 | 47.95 | 50.98 | 48.4 |
| $TiO_2$ | 0.05 | 0.04 | 0.09 | 0.05 | 0.05 | 0.04 | 0.04 | 0.07 | 0.03 | 0.07 | 0.06 |
| $Al_2O_3$ | 36.3 | 35.9 | 26.21 | 27.67 | 34.5 | 34.04 | 32.84 | 30.3 | 33.95 | 32.56 | 33.82 |
| FeO | 0.78 | 0.44 | 0.89 | 0.49 | 0.88 | 0.83 | 0.83 | 0.95 | 0.58 | 0.88 | 0.76 |
| MnO | 0.02 | 0.04 | 0.04 | 0.01 | 0.02 | 0.04 | 0.04 | 0.05 | 0.02 | 0.04 | 0.05 |
| MgO | 0.1 | 0.06 | 0.17 | 0.03 | 0.15 | 0.12 | 0.12 | 0.15 | 0.08 | 0.09 | 0.09 |
| CaO | 18.86 | 18.23 | 9.34 | 9.82 | 17.98 | 17.5 | 16.61 | 13.7 | 17.19 | 15.31 | 16.79 |
| $Na_2O$ | 0.71 | 1.24 | 5.09 | 5.24 | 1.23 | 1.59 | 1.75 | 3.22 | 1.47 | 2.54 | 1.78 |
| $K_2O$ | 0.05 | 0.08 | 1.79 | 0.99 | 0.07 | 0.09 | 0.18 | 0.46 | 0.13 | 0.32 | 0.18 |
| SUM | 103.12 | 103.60 | 101.26 | 101.12 | 102.78 | 102.25 | 100.66 | 100.36 | 101.39 | 102.79 | 101.93 |
| AN | 0.936 | 0.890 | 0.502 | 0.507 | 0.889 | 0.858 | 0.839 | 0.700 | 0.865 | 0.768 | 0.838 |

Analyses used a general silicate standardization which produces slightly high sums for magnesian olivines and orthopyroxenes. Types are r, rim analysis; c, core analysis; s, analysis of a small grain; g, analysis of a groundmass mineral; x, an analysis of a xenocryst; and m an analysis of a medium-grained crystal.. Analyses not marked by a g are of phenocrysts

AVP must then represent differences in the parental melts supplied to each volcanic center. Parental melts for volcanos in most of the Mariana Arc are derived principally from the mantle wedge [*Stern*, 1979; *Meijer and Reagan*, 1981; *Dixon and Stern*, 1983; *Dixon and Batiza*, 1979; *Woodhead and Fraser*, 1985]. It has been argued for both the islands and seamounts in the CIP and SSP [e.g. *Stern*, 1979, 1981; *Stern and Bibee*, 1984; *Dixon and Stern*, 1983; *Stern et al.*, 1988*a*] as well as for the seamounts discussed here [*Lin et al.*, this issue] that the melting of the wedge is in the spinel peridotite stability field. Extracting melts with diverse incompatible-element concentrations from such a peridotite requires either different degrees of melting of a homogeneous source or melting of a source with heterogeneous incompatible-element abundances.

For illustration we have calculated the relative effects of melting a homogeneous spinel peridotite from 2% to 30%. Both simple batch melting and fractional melting (with 3% melt retained in the depleted source) models were calculated. Initial modal mineral proportions and modal melting proportions are those used by *Lin et al.* [this issue]. Partition coefficients are listed in Figures 9 and 11. We have assumed that there is no residual Ti-bearing phase during melting. Recent experimental work [*Green and Pearson*, 1986; *Watson and Ryerson*, 1986] has shown that such phases are unlikely to persist at even slight degrees of partial melting.

Progressive melting produces melts with decreasing abundances of incompatible elements like Zr and Ba. Highly incompatible elements (Rb, K, Ba) will not fractionate so K/Rb and Rb/Ba will be relatively constant. Y and Zr have low, but significant partition coefficients in pyroxenes, so at low degrees of melting, K/Zr, Ba/Zr, and Ba/Y in the melts will be higher than in the source and will decrease with increasing degrees of partial melting (Figure 11). Y/Zr and Ti/Zr will increase slightly with increasing degrees of partial melting (Figure 11).

The patterns of element ratios and abundances in the most mafic samples from the Mariana and Volcano arcs are consistent, in a general way, with partial melting of a homogeneous source (Figure 11). The subalkalic samples from the CIP and southern NSP could represent a higher degree of melting than the alkalic samples. They have lower abundances of the LIL elements, lower K/Zr and Ba/Y, higher Y/Zr, and similar K/Ba and Ba/Rb [*Lin et al.*, this issue] compared with the alkalic samples, consistent with derivation by higher degrees of partial melting. The element abundances in the model source were arbitrarily set so that 30% melting produced compositions in the middle of the subalkalic field. The K-rich samples then represent about 2-10% melting. The production of primary, subalkalic arc basalts has been suggested to actually require 6 to 15% melting of peridotite [*Stern and Bibee*, 1984; *Green*, 1971] which would require that the alkalic samples represent about 1-5% melting of the same source as that producing the subalkalic volcanics.

There are, however, some problems with this simple an interpretation. The fractionation of K and Ba from Zr requires residual CPX during melting. The same residual CPX produces very low Sc abundances in the resulting melts (Figure 11), much lower than are observed in the magnesian alkalic basalts. Low percent partial melting of peridotite produces very magnesian, Si-undersaturated, alkali-olivine basalts [*Jacques and Green*, 1980]. These are not typical of the AVP. which has marginally undersaturated magnesian basalts. More telling is evidence from rare earth element and isotopic determinations. The AVP lavas are characterized by high La/Yb and low Ba/La [*Lin et al.*, this issue]. Though low degrees of melting can produce the former [*Lin et al.*, this issue] it should also produce higher Ba/La ratios,

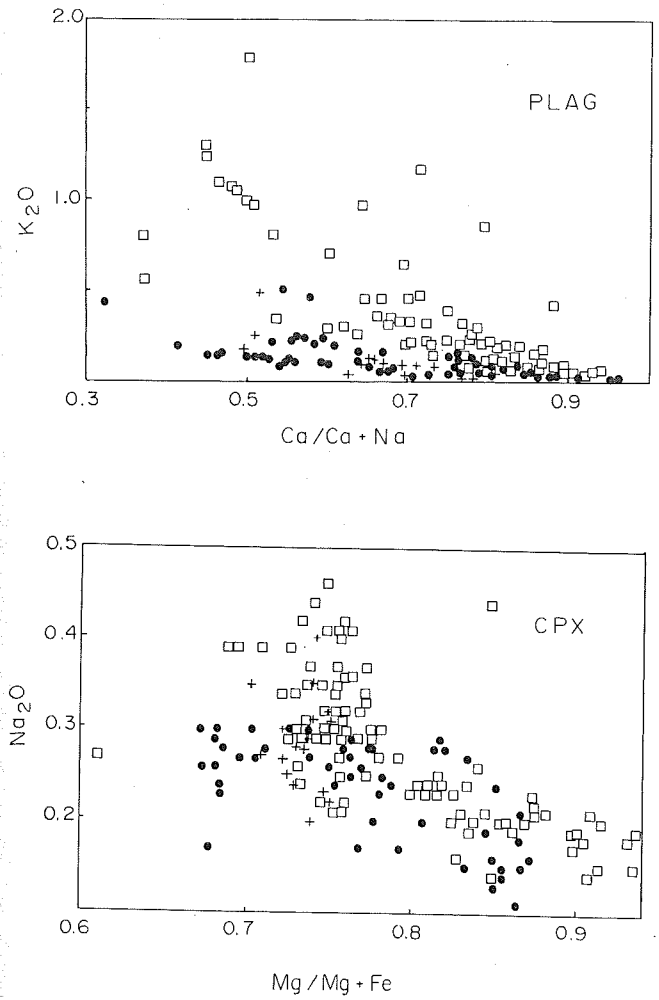


Fig. 8. Mineral compositions in Mariana-Volcano Arc lavas. Symbols as in Figure 2. (Top) Plagioclase phenocrysts, (Bottom) Clinopyroxene phenocrysts. Oxides in weight percent. Ca/Ca+Na and Mg/Mg+Fe in molar proportions.

if CPX is a residual phase. The very low Ba/La of the AVP lavas compared with those of the Volcano Arc and CIP indicate a fundamental difference in the sources for the alkalic and subalkalic lavas. This is consistent with differences in Nd and Sr isotopic compositions between lavas from the two suites [*Lin et al.*, 1988]. Lowered degrees of partial melting alone are not an adequate mechanism to produce the two groups of lavas in the Mariana-Volcano Arc, though variations in degree of melting may contribute to the diversity of lavas in the region.

The enrichment in the source for the AVP lavas is in K, Rb, Ba, Sr, and the LREE. The range of mantle variations necessary to produce the range in parental compositions can be produced by mixing of two end-members, one with Ba/La = 80 and $(La/Yb)_n$ = 0.5, and the other with Ba/La = 20 and $(La/Yb)_n$ = 15 [*Lin et al.*, this issue]. The latter is similar to the mantle source producing volcanism in the Caroline hotspot [*Stern*, 1981], while the former may represent a slab-derived component. If the depletions in high-field strength (HFS) and heavy rare earth elements (HREE) characteristic of all of these arc lavas are a result of melting of a once-depleted mid-ocean ridge basalt source, the metasomatism affecting that MORB source before its melting to make arc tholeiites must include a component from both the slab and an ocean island basalt source, though one component or the other may dominate in different parts of the arc [*Lin et al.*, this issue].

### *Tectonic Setting and Alkalic Arc Volcanism*

The existence of a major province of alkalic volcanism along the magmatic front of an intraoceanic arc is unusual [*DeLong et al.*, 1975]. The alkalic volcanics are, in fact, most similar to rocks of the shoshonitic series. These are defined as rocks with moderate Fe enrichment, low Ti contents, near silica saturation, high total alkali contents (3-4% at 46% $SiO_2$,7-8% at 54.5% $SiO_2$) and high K/Na (>0.6 at 50% $SiO_2$, >1.0 at 55% $SiO_2$ [*Morrison*, 1980]). Samples from Fukutoku (55-1-2), Central Hiyoshi (52-1-1,1-4,1-5), and North Hiyoshi (53-1-2) are all shoshonites by the criteria of *Morrison* [1980]; 55-1-2 can be termed an absarokite and 53-1-2 a banakite [*Joplin*, 1968]. South Hiyoshi includes shoshonites by the criteria of *Joplin* [1968].

The shoshonitic rock association has been reported in a variety of settings in island arcs and continental arcs. In Fiji, the youngest rocks in the arc sequence are shoshonitic, succeeding tholeiitic and calcalkalic lavas [*Gill* 1970]. High-K shoshonitic rocks are among the youngest eruptives in the Eolian Arc [*Barberi et al.*, 1973]. In southern Peru and the Sunda Arc there is a zonation in erupted rock type away from the subduction zone from tholeiitic to calcalkaline to shoshonitic [*Whitford and Nicholls*, 1976; Lefevre, 1973]. *Jakes and White* [1972] and later, *Morrison* [1980], have suggested that in general the arc shoshonitic suite is intimately associated with calcalkaline volcanics, that in a spatially zoned suite of arc lavas the shoshonitic rocks occur above the deeper part of the Benioff zone, and that in areas without a spatial zonation of shoshonites, they are younger and associated with oblique convergence, possibly related to steepening of the Benioff zone.

The AVP volcanos do indeed lie near a major bend in the Bonin-Mariana Trench, along which convergence must have a large oblique component [*Eguchi*, 1984]. There are, however, two other aspects of their tectonic setting which may bear on the problem of shoshonitic production. First, the volcanos are just south of the point at which the Michelson Ridge, a large intraplate volcanic ridge whose western end is the Ogasawara Plateau, is being subducted beneath the Bonin Trench. This ridge may have caused the bend in the trench system [*Vogt et al.*, 1976; *McCabe*, 1984]. Second, Iwo Jima sits immediately north of the termination of the Mariana Trough, and the unusual lava compositions of the AVP have been argued to result from the propagation of the back-arc spreading center into the arc [*Stern et al.*, 1988b]. We will examine in turn the possible effects of oblique subduction, seamount subduction, and back arc propagation on the origin of the alkalic volcanism.

Though Morrison has noted that the shoshonitic association may be related to the effects of oblique convergence, it does not appear to be a sufficient condition for such volcanism. The southern Mariana Trench, a trench-trench transform, is also undergoing highly oblique convergence, but despite this oblique subduction there is no evidence in the southern seamount province of alkali-enriched shoshonitic volcanism [*Dixon and Stern*, 1983; *Stern et al.*, 1988*a*]. In addition, if the shoshonitic volcanism associated with Iwo Jima were related to a tear or a deepening of the Benioff Zone due to oblique subduction, we would expect a geochemical anomaly symmetrical about the zone of that oblique convergence. One of the peculiar features of the geochemical enrichment in the northern NSP and southern Volcano Arc is that it seems to be asymmetric. This is most

TABLE 4. Results of Least Squares Major Element Modeling

| | Cheref | | | | Ahyi | | South Daikoku | | Central Hiyoshi | |
|---|---|---|---|---|---|---|---|---|---|---|
| | 1 | 2 | 3 | 4 | 5 | 6 | 7 | 8 | 9 | 10 |
| Parent | 9-6 | 10-2-7 | 10-2-7 | 10-2-7 | 15-3-3 | 15-3-3 | 25-8 | 25-8 | 52-1-1 | 52-1-1 |
| Daughter | 9-20 | 10-2-11 | 10-1-2 | 9-6 | 15-3-2 | 16-3 | 25-1 | 25-18 | 51-3 | 52-3-1 |
| Type | A | A | F | A | F | A | F | F | A | A |
| $r^2$ | 0.04 | 0.05 | 0.02 | 0.21 | 0.003 | 1.25 | 0.08 | 0.05 | 0.54 | 0.32 |
| F | 87.6 | 51.9 | 54.6 | 65.4 | 75.9 | 46.2 | 56.1 | 66.2 | 51.3 | 79.1 |
| PLAG | 10.5 | 35.8 | 28.8 | 16.9 | 13.8 | 14.9 | 23.9 | 19.9 | 38.8 | 18.1 |
| OL | 1.9 | 2.8 | - | 6.8 | 1.3 | 9.8 | - | - | - | - |
| CPX | - | 5.1 | 5.1 | 10.0 | 3.2 | 29.1 | 12.3 | 9.5 | 7.1 | 1.8 |
| OPX | - | - | 9.0 | - | 4.5 | - | 5.4 | 3.4 | - | - |
| SP | - | 4.4 | 2.6 | 1.0 | 1.3 | - | 2.3 | 1.1 | 2.8 | 1.0 |
| CPX/PLAG | - | 0.1 | 0.2 | 0.6 | 0.2 | 0.6 | 0.5 | 0.5 | 0.2 | 0.1 |

| | Nikko | | | | North Hiyoshi | Kaitoku | | Nishinoshima | Low-K to High-K | |
|---|---|---|---|---|---|---|---|---|---|---|
| | 11 | 12 | 13 | 14 | 15 | 16 | 17 | 18 | 19 | 20 |
| Parent | 45-1 | 45-1 | 45-1 | 45-1 | 54-1-3 | 77-13 | 75-4 | 80-1 | 8-3 | 16-3 |
| Daughter | 45-11 | 45-2 | 45-8 | 46-5-1 | 53-1-2 | 75-4 | 77-5 | 79-3 | 54-1-3 | 54-1-3 |
| Type | F | A | A | A | F | F | A | F | F | F |
| $r^2$ | 0.29 | 0.62 | 0.06 | 0.39 | 0.14 | 0.01 | 0.04 | 0.004 | 0.07 | 0.005 |
| F | 33.0 | 91.5 | 55.0 | 30.7 | 24.3 | 16.1 | 61.5 | 71.5 | 35.9 | 27.6 |
| PLAG | 31.8 | 8.5 | 21.9 | 37.4 | 39.8 | 46.7 | 31.4 | 14.1 | 22.3 | 24.8 |
| OL | - | - | 4.9 | 5.9 | 6.8 | 10.3 | 4.6 | 3.9 | 5.7 | - |
| CPX | 24.2 | - | 15.0 | 23.4 | 22.5 | 22.6 | 2.5 | 8.9 | 28.1 | 32.6 |
| OPX | 3.2 | - | - | - | - | - | - | - | 8.1 | 12.5 |
| SP | 7.6 | - | 3.3 | 2.6 | 6.6 | 4.3 | - | 1.5 | - | 2.4 |
| CPX/PLAG | 0.8 | - | 0.7 | 0.6 | 0.6 | 0.5 | 0.1 | 0.6 | 1.3 | 1.3 |

Under type, A indicates a crystal accumulation model (parent + crystals = daughter) and F indicates a fractionation model (parent - crystals = daughter); $r^2$ is the sum of residuals in the least squares calculation, and F is the fraction of liquid mixed or remaining. Mineral abbreviations are as in Table 2.

clearly shown in Ba abundances (Figure 4). The enrichments (which are extreme in Iwo Jima) extend southward at least two degrees, while to the north they stop abruptly in the northern Volcano Arc north of 25°N. Such a distribution seems more consistent with a source which is moving to the north relative to the Volcano Arc than to a static anomaly associated with a zone of oblique convergence.

The subduction of the Michelson Ridge might provide a source for incompatible-element enrichments. If it is similar to other intraplate seamounts, it is in part alkalic, and enriched in LREE, Ba, Sr, and K, as well as Ti, Zr and Y [*Stern*, 1981]. It is not clear, however, that the trace of the Michelson Ridge has ever been beneath the mantle now contributing to volcanism in the AVP. Iwo Jima and the rest of the AVP are over 100 km south of the ridge-trench collision. The trend of the Michelson Ridge is about 290°, while convergence is at about 280° [*Eguchi*, 1984]. Depending upon the rate of convergence assumed, this means that the collision zone has been near stationary, or moving south at 10-20 km/m.y., which suggests that the trace of the ridge has never been beneath Iwo Jima. It should also be noted that despite the large number of intraplate seamounts on the offshore slope, none of the rest of the arc is erupting alkalic

The third possibility concerns the interaction of a propagating back arc rift with the Volcano Arc [*Stern et al.*, 1984]. If the

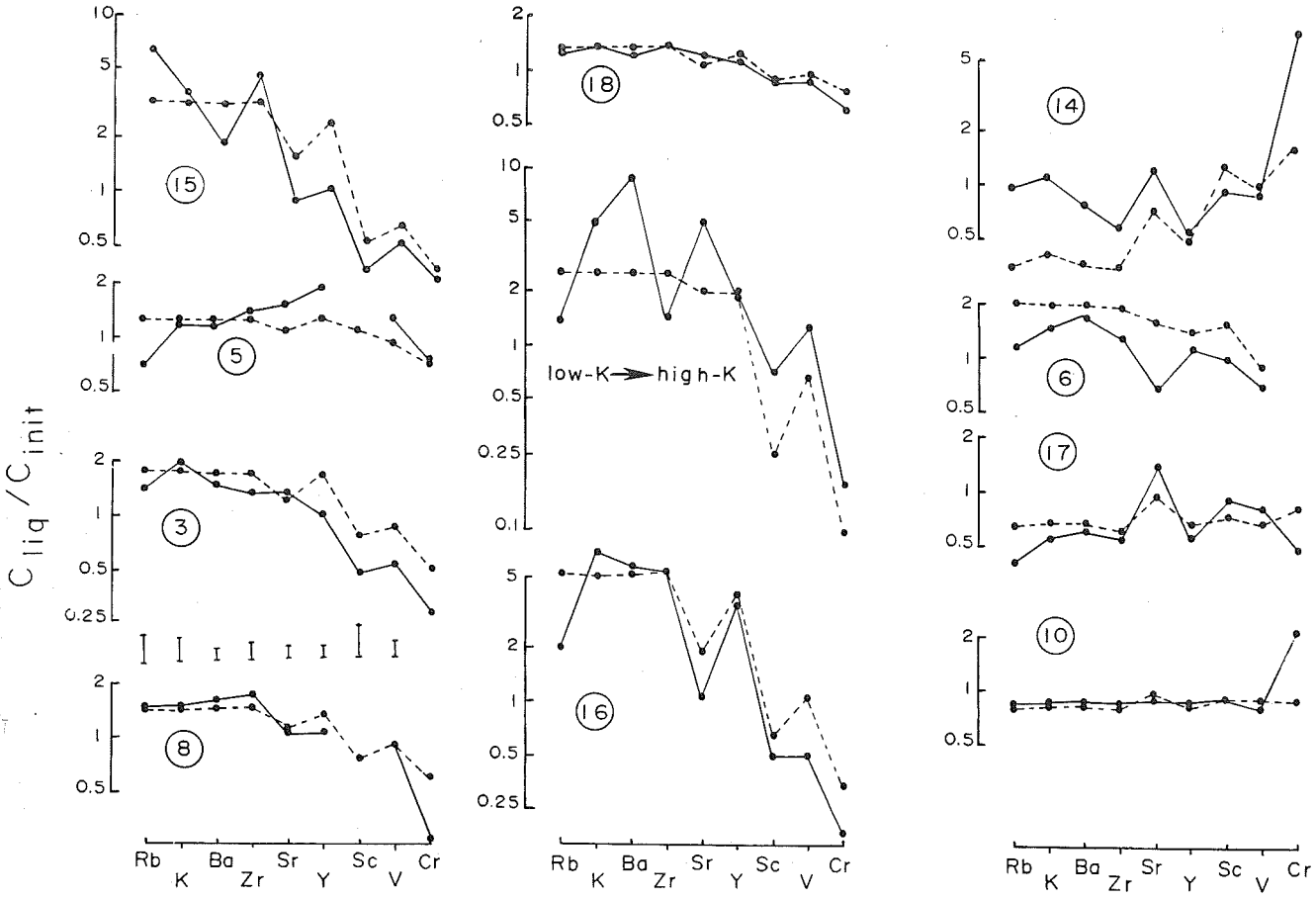


Fig. 9. Results of trace element modeling for crystal fractionation and accumulation. Solid lines are ratios of measured values in daughter compositions over values in the parent compositions. Dashed lines are calculated trace element compositions from the major element models over the measured values in the parent composition. Numbers correspond to the major element models of Table 4. The bars above number 8 are approximate errors for about 20% fractionation of a low-K, subalkalic sample. The figure labeled low-K to high-K is for the derivation of a high-K basalt from a low-K basalt by high-pressure crystallization (model 19 in Table 4). Number 20 in Table 4 yields a similar result. Note the general similarity of calculated and measured patterns (excepting models 6 and 14). Simple Rayleigh fractionation was assumed ($C_{liq}/C_o = F^{D-1}$, where F is the fraction of liquid remaining, D the bulk partition coefficient, and $C_{liq}$ and $C_o$ the final and initial element concentrations, respectively). Partition coefficients for PLAG were Rb = 0.14, K = 0.16, Ba = 0.16, Sr = 1.1, Y = 0.06, V = 0.02, Cr = 0.04; for CPX were Zr = 0.12, Sr = 0.10, Y = 0.7, Sc = 4.0, V = 2.0, Cr = 5.0; for OPX Zr = 0.1, Y = 0.18, Sc = 4.0, V = 3.0, Cr = 7.2; for OL were Y = 0.07, V = 0.04, Cr = 1.4, and for magnetite were Zr = 0.4, Y = 0.2, Sc = 3.0, V = 8.0, and Cr = 1.0. Other partition coefficients were taken at 0.01. Crystal accumulation models were calculated by mass balance.

back arc rift is moving northward, the southern portions of the Volcano Arc are undergoing extension, as presumably is the entire upper part of the crust and mantle. Such rifting may contribute to enhanced mantle diapirism and may expose deeper levels of the mantle which have not been previously melted. If the mantle is fundamentally veined, with an enriched component in a depleted matrix, the onset of back arc rifting may thus "unroof" deeper portions of the mantle which have not yet been exhausted of their enriched component by arc melting. As back arc rifting proceeds, the arc volcanos move further from the rift axis, their mantle source becomes more depleted, and the signal of this rifting starts to decay. Eventually the arc lavas erupted in these centers return to the compositions they had before the episode of back arc rifting.

If the province of alkalic volcanism is related to back arc rifting, there should be a cycle of volcanism from prerift tholeiitic or calcalkalic volcanism, interrupted by an alkalic phase during the onset of back arc spreading, followed by a progressive return with time to tholeiitic or calcalkalic compositions after rifting. Indeed the volcanos north and south of this proposed propagating zone in the Marianas are tholeiitic or calcalkalic. The active volcanos near the rift tip, and the most recently reestablished arc volcanos are all erupting principally alkalic compositions. Minami Iwo Jima, the only large, extinct volcano in the AVP, is subalkalic and may represent the prerift phase of volcanisms. The only other extinct edifice in the AVP is a very small alkalic seamount (Fukutoku). It is not large enough to have been active very long and was likely part of the Hiyohsi-Iwo Jima volcanism.

The decay of this alkalic volcanism southward down the Mariana Arc, if it is a decay, is not smooth. Nikko, immediately south of the AVP, has very depleted subalkalic compositions. There is, however, another province of alkali-enriched volcanism at 21° to 22°N (Daikoku, Eifuku, Fukujin), though these lavas

TABLE 5. Average Compositions of Least Fractionated Basalts (Cr > 100 ppm) From Each Seamount Province.

| | CIP | | SNSP | | AVP | | KITA IWO |
|---|---|---|---|---|---|---|---|
| | av | sd | av | sd | av | sd | |
| $SiO_2$ | 49.89 | 3.17 | 50.39 | 1.51 | 48.65 | 0.23 | 43.36 |
| $TiO_2$ | 0.69 | 0.19 | 0.69 | 0.11 | 0.77 | 0.03 | 0.65 |
| $Al_2O_3$ | 15.85 | 1.83 | 14.94 | 1.13 | 15.70 | 0.32 | 15.29 |
| $FeO^t$ | 9.60 | 0.85 | 9.38 | 0.35 | 9.29 | 1.19 | 10.15 |
| MnO | 0.20 | 0.03 | 0.18 | 0.01 | 0.25 | 0.07 | 0.20 |
| MgO | 9.12 | 1.98 | 8.46 | 0.56 | 8.17 | 0.67 | 12.04 |
| CaO | 12.46 | 1.76 | 11.69 | 0.33 | 11.80 | 0.57 | 14.15 |
| $Na_2O$ | 1.79 | 0.52 | 1.86 | 0.35 | 1.97 | 0.25 | 1.16 |
| $K_2O$ | 0.44 | 0.27 | 0.70 | 0.28 | 1.56 | 0.68 | 0.31 |
| $P_2O_5$ | 0.12 | 0.02 | 0.11 | 0.02 | 0.26 | 0.11 | 0.08 |
| SUM | 100.16 | | 98.43 | | 98.43 | | 97.39 |
| # | 3 | | 3 | | 3 | | 1 |
| Rb | 12.3 | 4.0 | 18.0 | 6.1 | 23.3 | 17.3 | 3 |
| Sr | 259.0 | 35.0 | 396.3 | 110.9 | 809.3 | 132.6 | 432 |
| Ba | 94.0 | 46.0 | 213.3 | 45.6 | 492.3 | 110.1 | 89 |
| Zr | 22.0 | 22.0 | 25.0 | 7.0 | 54.0 | 15.0 | 11 |
| Y | 13.8 | 6.2 | 14.3 | 3.7 | 15.3 | 3.3 | 9 |
| Sc | 50.0 | 9.2 | 48.5 | 1.5 | 40.2 | 4.9 | 26 |
| V | 291.0 | 5.7 | 260.7 | 52.1 | 268.3 | 20.0 | 369 |
| Cr | 238.0 | 106.0 | 184.3 | 46.0 | 186.5 | 32.1 | 166 |
| Ni | 76.0 | 40.0 | 39.7 | 28.7 | 65.3 | 18.1 | 22 |
| Cu | 96.0 | 12.0 | 120.3 | 13.8 | 116.0 | 22.4 | 90 |
| $K_2O+Na_2O$ | 2.23 | | 2.56 | | 3.53 | | 1.47 |
| $K_2O/Na_2O$ | 0.25 | | 0.38 | | 0.79 | | 0.27 |
| $CaO/Al_2O_3$ | 0.79 | | 0.78 | | 0.75 | | 0.93 |
| Ti/Zr | 188.03 | | 166.26 | | 85.30 | | 354.25 |
| Ba/Zr | 4.27 | | 8.53 | | 9.12 | | 8.09 |
| Ba/Y | 6.81 | | 14.88 | | 32.11 | | 9.89 |

The Kita Iwo Jima sample has clearly accumulated CPX phenocrysts but it is included for comparison as it is the only magnesian compostion available from the Volcano Arc. av indicates the average of analyses of magnesian samples, sd their standard deviation.

are not as enriched as those of the AVP [*Lin et al.*, this issue, Figure 11]. Lavas from volcanos south of this province are again rather low-K volcanics. This irregular decay suggests that the production of shoshonitic lavas during back arc rifting may be some what episodic.

One of the interesting observations about the Eifuku-Fukujin region is that the only other shoshonitic lavas reported in the Mariana Arc are found on a cross-chain volcano near Fukujin. This volcano, South Kasuga, is just south of Fukujin [*Jackson and Fryer*, 1986), west of the magmatic front volcanos which have been discussed in this paper, and is closer to the locus of back arc spreading than those volcanos. The occurrence of shoshonitic lavas in at least one of the cross-chain volcanos reinforces the idea that proximity to an active back arc rift may promote alkalic arc volcanism.

The existence of a nascent back arc basin may not in itself be sufficient to produce shoshonitic volcanism. There are several narrow basins west of the Volcano-Izu Arc from Nishino-shima northward which have been interpreted as incipient back arc basins [*Yuasa*, 1985; *Honza and Tamaki*, 1985]. None of the arc volcanos on the Shichito Ridge, including Nishino-shima, have however, erupted high-K basalts. There may be additional conditions required to effect the link between shoshonitic volcanism and back arc rifting: perhaps a threshold rate of back arc rifting or propagation or the coincidence of back arc rifting and oblique subduction.

The northern Mariana Arc and Volcano Arc are not the only cases of alkalic arc volcanism associated with back arc rifting. In the Vanuatu arc, LIL-enriched, low-$TiO_2$ basalts have been erupted on Ambrym, which lies at the southern closure of a back arc basin that has been opening since the Pleistocene [*Gorton*, 1977; *Carney and McFarlane*, 1982]. Like Iwo Jima and the Michelson Ridge, Ambrym lies near the intersection of the trench and the D'Entrecasteaux Fracture Zone, suggesting that there may be a link between aseismic ridge collisions, back arc rifting, and alkalic arc volcanism [*Vogt et al.*, 1976; *DeLong et al.*, 1975]. There are also sodic alkaline basalts on Penguin Island off the Antarctic Peninsula which appear to be associated with the early stages of back arc opening in the Bransfield Strait [*Tarney et al.*, 1982].

The fundamental link between shoshonitic associations in different arcs may not be a particular tectonic regime, but simply

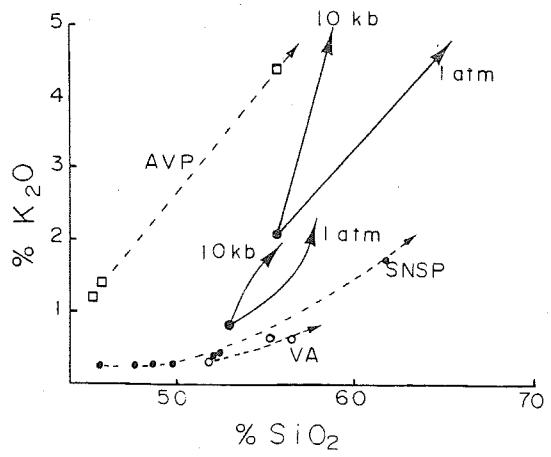


Fig. 10. $K_2O$ versus $SiO_2$ variations for fractionation of shoshonitic lavas from low-K compositions. The 1-atm and 10-kbar lines are experimental results on a low-K and high-K starting composition [*Meen*, 1987]. The early crystallization of OPX at 10 kbar produces extreme K enrichment with little enrichment in Si. Note that the fractionation trends of AVP lavas do not parallel those of the 10-kbar experiments and that the AVP and SNSP lavas do not track back to similar compositions.

any tectonic regime which allows access to a deeper and more enriched part of the mantle. Such tectonic regimes could include oblique subduction zones, arcs undergoing extension, or volcanism over a particularly deep Benioff zone with a consequently thick mantle wedge.

*Implications for Arc Evolution*

Alkali-element variations in Mariana arc lavas have been discussed in two contexts. The first was a model suggesting that smaller islands and seamounts in the arc tend to be more alkali-enriched [*Dixon and Batiza*, 1979], and the second was a model postulating that the early phases of the evolution of an arc volcano may be characterized by an alkalic phase [*Meijer and Reagan*, 1983].

There is no clear correlation in our data, within a given volcanic province, for the smaller edifices to be more potassic or higher in total alkali contents than the larger (Figure 12). The relationship between alkali enrichment and arc evolution would seem to be less one of the evolution of an individual volcano than of the evolution of provinces within the arc. In the CIP, with a least a few million years of evolution since back arc opening, both small and large edifices within a region span

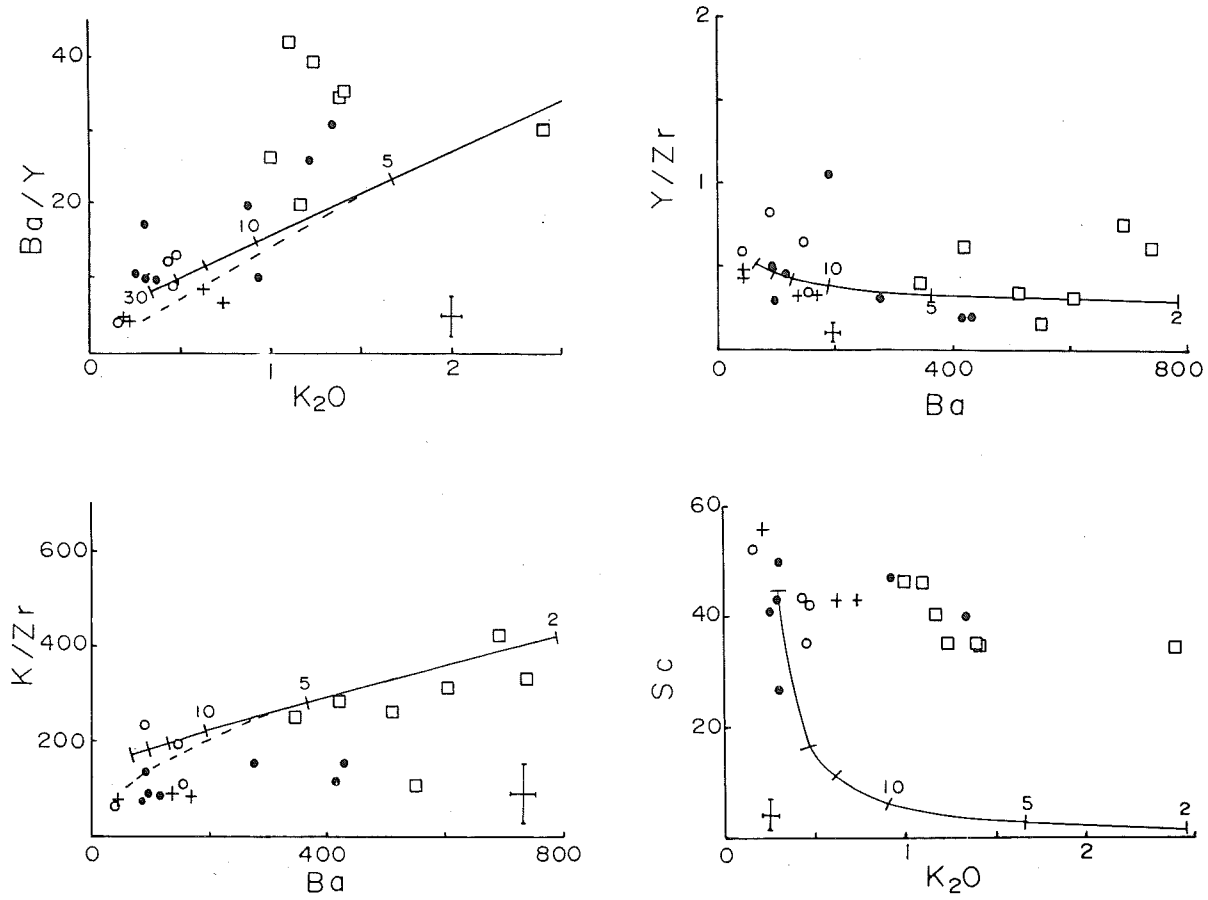


Fig. 11. Results of spinel peridotite partial melting modeling. Solid line is for batch melting (marked at 2, 5, 10, 15, 20 and 30% melting). Dotted line is for a fractional melting model with 3% melt retained in the solid residue. The second model is plotted only where it dverges from the first. Symbols are as in Figure 2, but only samples with over 6% MgO are plotted. Error bars are calculated for subalkaline samples with low abundances of Ba and K. Initial modal mineral abundances and modal melting abundances are from *Lin et al.* [this issue]. Equation for batch melting was $C_{liq}/C_o = 1/F + D(1 - F)$, where the variable are defined as in Figure 9. $C_o$ values were arbitrarily taken so that 30% partial melting produced values in the subalkalic (CIP and SNSP) basalt field. Partition coefficients are those used in Figure 9 with the addition of spinel partition coefficients of Zr = 0.4, Y = 0.2, Sc = 3.0, V = 8.0, and Cr = 1.0.

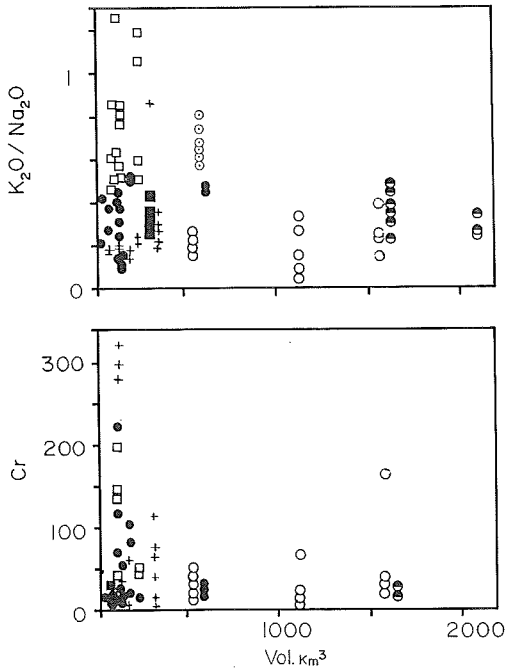


Fig. 12. Cr (in ppm) and $K_2O/Na_2O$ versus volume for each edifice. Symbols as in Figure 2. Volumes from *Bloomer et al.* [1989].

similar compositional ranges. In the AVP the volcanos are in a transition between the cessation of volcanism on the West Mariana Ridge and the inception of volcanism along the northern Mariana Arc. The small size of the Hiyoshi Seamounts may be a consequence of very recent rifting of the arc [*Stern et al.*, 1984; 1988*b*] or a consequence of very slow opening and hence magmatic evolution at these latitudes.

The idea of *Meijer and Reagan* [1983] may, in a way, be correct. The waning and incipient stages of arc volcanism associated with the development of a back arc basin may be characterized by alkalic volcanism. As the arc matures, and the back arc basin widens, the arc erupts principally subalkaline tholeiitic or calcalkalic lavas, and any new volcanos initiated along the arc have compositions typical of the particular province in which they occur.

One of the few characteristics that may be associated with volume is the frequency of occurrence of less-fractionated lavas. Less-fractionated compositions, whether judged by Cr, Ni, or MgO contents, are more common in the smaller submarine edifices described here (Figure 12). This is not to say that magnesian lavas are restricted to the smaller volcanos. Pagan, the second largest island in the Marianas, includes basalts with 11.4% MgO [*Meijer*, 1982], and South Kasuga Seamount (500 $km^3$) has basalts with 10% MgO [*Jackson and Fryer*, 1986]. There is, however, a clear tendency for the less-fractionated lavas to occur more frequently in the small edifices. Volcanos larger than about 400 $km^3$ more typically erupt only quite fractionated lavas (Cr < 50 ppm) when sampled. This suggests that in the smallest edifices, which probably are built on the thinnest crust and perhaps have the shortest lived chambers, magnesian melts are more commonly erupted. Past a certain size, the crustal thickness of the arc edifice results in greater fractionation of melts prior to eruption. The smaller edifices do erupt fractionated compositions, similar to those seen in the larger volcanos; the difference is that the small volcanos more often allow more magnesian melts to the surface.

## Conclusions

The Mariana-Volcano Arc is characterized by two rock series, one subalkalic and the other alkalic. The former characterizes volcanos in the Central Island Province, the southern Northern Seamount Province, and the northern Volcano Arc. These lavas include both low-K and medium-K series, range from basalts to andesites and dacites, and have anhydrous phenocryst assemblages dominated by plagioclase. The alkalic association occurs only in the Northern Seamount Province and southern Volcano Arc and is a shoshonitic series characterized by enrichments in K, K/Na, Rb, Ba, and Sr relative to the other volcanic suites. These differences are not related to degree of fractionation or the size of the edifices. Islands and seamounts within each province have similar compositions; there is however a tendency for the most magnesian samples to come from the smallest edifices.

The intra-edifice variations in both the alkalic and subalkalic groups can, for the most part, be accounted for by 10% to 80% crystallization of PLAG-OL-CPX with small amounts of OPX and titanomagnetite. The differences between edifices may be in part due to differences in degree of melting (1-5% for the alkalic province versus 10-15% for the subalkalic province), but some element abundances and ratios, as well as preliminary isotopic data, require a distinct difference in the sources producing parental magmas in the two provinces. The characteristics of this source (low Ba/La, high Ba/Zr) may be a consequence of the subduction of large intraplate ridges or of the uncovering of a less-depleted mantle source by the propagation of the Mariana Trough spreading center into the Volcano Arc.

*Acknowledgments.* We thank the officers and crew of the R/V *Thomas Thompson* for enthusiastic and professional work in the collection of these samples. K. Nilsson assisted with several of the rock analyses and microprobe analyses. T. Sohlburg of VPI assisted with the microprobe work. The manuscript was greatly improved by careful reviews from J. Gill, A. Meijer, and S. Box. This work was supported by NSF grants OCE-8415739 to S. H. Bloomer and OCE-8415699 to R. J. Stern.

## References

Barberi, F., P. Gasparinit, F. Innocenti, and L. Villari, Volcanism in the southern Tyrrhenian Sea and its geodynamic implications, *J. Geophys. Res., 78*, 5221-5232, 1973.

Barberi, F., F. Innocenti, G. Ferrara, J. Keller, and L. Villari, Evolution of Aeolian arc volcanism, *Earth Planet. Sci. Lett., 21*, 269-271, 1974.

Bloomer, S., R. J. Stern, and N. C. Smoot, Physical volcanology of submarine volcanos in the northern Mariana and southern Volcano Arcs, in press, *Bull. Volcanol.*, 1989.

Carney, J. N., and A. MacFarlane, Geologic evidence bearing on the Miocene to Recent structural evolution of the New Hebrides, *Tectonophysics, 87*, 147-175, 1982.

Chase, T. E., H. W. Menard, and J. Mammerickx, Bathymetry of the North Pacific, Chart #6, *Inst. Mar. Res. Tech. Rep. Series TR-11*, 1968.

DeLong S. E., F. N. Hodges, and R.J. Arculus, Ultramafic and mafic inclusions, Kanaga Island, Alaska, and the occurrence of alkaline rocks in island arcs, *J. Geol., 83*, 721-736, 1975.

deVries Klein, G., and K. Kobayashi, Geological summary of the north Philippine Sea, based on Deep Sea Drilling Project leg 58 results, *Initial Rep. Deep Sea Drill. Proj., 58*, 951-970, 1980.

Dixon, T. H., and R. Batiza, Petrology and chemistry of recent lavas in the Northern Marianas: Implications for the origin of island arc basalts, *Contrib. Mineral. Petrol., 70*, 167-181, 1979.

Dixon, T. H., and R. J. Stern, Petrology, chemistry and isotopic

composition of submarine volcanoes in the southern Mariana arc, *Geol. Soc. Am. Bull., 94*, 1159-1172, 1983.

Eguchi, T., Seismotectonics around the Mariana Trough, *Tectonophysics, 102*, 33-52, 1984.

Fryer, P., Morphology of seamounts in the Mariana island arc system, *Eos, Trans. AGU, 66*, 421, 1985.

Garcia, M. O., N. W. K. Liu, and D. W. Muenow, Volatiles in submarine volcanic rocks from the Mariana Island arc and trough, *Geochim. Cosmochim. Acta, 43*, 305-312, 1979.

Gill, J. B., Geochemistry of Vitu Levu, Fiji and its evolution as an island arc, *Contrib. Mineral. Petrol., 27*, 179-203, 1970.

Gill, J. B., *Orogenic Andesites and Plate Tectonics*, 390 p.,Springer Verlag, Berlin, 1981.

Gorton, M. F., The geochemistry and origin of Quaternary volcanism in the New Hebrides, *Geochim. Cosmochim. Acta, 41*, 1257-1270, 1977.

Green, D. H., Composition of basaltic magmas as indication of conditions of origin: Application to ocean floor volcanism, A discussion of the petrology of igneous and metamorphic rocks from the ocean floor, *Philos. Trans. R. Soc. London Ser. A, 268*, 707-725, 1971.

Green, T. H., and N. J. Pearson, Ti-rich accessory phase saturation in hydrous mafic-felsic compositions at high P, T, *Chem. Geol., 54*, 185-201, 1986.

Gust, D. A., and M. R. Perfit, Phase relations of a high-Mg basalt from the Aleutian Island Arc: Implications for primary island arc basalts and high-Al basalts, *Contrib. Mineral. Petrol., 97*, 7-18, 1987.

Hole, M. J., A. D. Saunders, G. F. Marriner, and J. Tarney, Subduction of pelagic sediments: implications for the origin of Ce-anomalous basalts from the Mariana islands, *J. Geol. Soc. London., 141*, 453-472, 1984.

Honza, E., and K. Tamaki, The Bonin Arc, in *The Ocean Basins and Margins*, vol. 7A, edited by. A. Nairn, F. Stehli, and S. Uyeda, pp. 459-502, Plenum, New York, 1985.

Hussong D. M., and P. Fryer, Back-arc seamounts and the SeaMARC II seafloor mapping system, *Eos Trans. AGU, 64*, 627-632, 1983.

Hussong D. M., and S. Uyeda, Tectonic processes and the history of the Mariana arc: A synthesis of the results of Deep Sea Drilling Project leg 60, *Initial Rep. Deep Sea Drill. Proj., 60*, 909-929, 1981.

Irvine, T. N., and W. R. A. Baragar, A guide to the chemical classification of the common volcanic rocks, *Can. J. Earth Sci., 8*, 523-548, 1971.

Jackson, M. C., and P. Fryer, The Kasuga volcanic cross-chain: A calc-alkaline basalt-dacite suite in the northern Mariana island arc, *Eos Trans. AGU, 67*, 1276, 1986.

Jacques, A. L., and D. H. Green, Anhydrous melting of peridotite at 0-15 kb pressure and the genesis of tholeiitic basalts, *Contrib. Mineral. Petrol., 73*, 287-310, 1980.

Jakes, P., and J. B. Gill, Rare earth elements and the island arc tholeiite series, *Earth Planet. Sci. Lett., 9*, 17-28, 1970.

Jakes, P., and A. J. R. White, Major and trace element abundance in volcanic rocks of orogenic areas, *Geol. Soc. Am. Bull., 83*, 29-39, 1972.

Joplin, G. A., The shoshonite association: a review, *J. Geol.lSoc. Australia, 15*, 275-294, 1968.

Kuno, H., *Catalogue of the Active Volcanos of the World Including Solfatara Fields, Part II, Japan, Taiwan, and Marianas*, International Association of Volcanology, Naples, 1962.

Kushiro, I., The system forsterite-diopside-silica with and without water at high pressures, *Am. J. Sci., 267A*, 269-294, 1969.

Lefevre, C., Les caracteres magmatiques du volcanisme Plio-Quaternaire des Andes dans le sud de Perou, *Contrib. Mineral. Petrol., 41*, 259-271, 1973.

Lin, P. N., R. J. Stern, J. Morris, E. Ito, and S. Bloomer, Constraints on melt sources for the northern Mariana and Southern Volcano Arcs: LIL, REE, Sr-, Nd-, Pb-, and O-isotopic data, *Eos Trans. AGU, 69*, 505, 1988.

Lin, P. N., R. J. Stern, and S. H. Bloomer, Shoshonitic volcanism in the northern Mariana Arc 2, Large-ion lithophile and rare earth element abundances: Evidence for the source of incompatible element enrichments in intraoceanic arcs, *J. Geophys. Res.*, this issue.

McCabe, R., Implications of paleomagnetic data on the collision related bending of island arcs, *Tectonics, 3*, 409-428, 1984.

Meen, J. K., Formation of shoshonites from calcalkaline basalt magmas: Geochemical and experimental constraints from the type locality, *Contrib. Mineral. Petrol., 97*, 333-351, 1987.

Meijer, A., Pb and Sr isotopic data bearing on the origin of volcanic rocks from the Mariana island-arc system, *Geol. Soc. Am. Bull., 87*, 1358-1369, 1976.

Meijer, A., Primitive arc volcanism and a boninite series: examples from western Pacific island arcs, in *The Tectonic and Geologic Evolution of Southeast Asian Seas and Islands Part 2*, Geophys. Monogr., edited by D. E. Hayes, pp. 255-269, AGU, Washington, D. C., 1980.

Meijer, A., Mariana-Volcano Islands, in *Andesites: Orogenic Andesites and Related Rocks*, edited by R. S. Thorpe, pp. 293-306, John Wiley, New York, 1982.

Meijer, A., and M. Reagan, Petrology and geochemistry of the island of Sarigan in the Mariana Arc: Calc-alkaline volcanism in an oceanic setting, *Contrib. Mineral. Petrol., 77*, 337-354, 1981.

Meijer, A., and M. Reagan, Origin of $K_2O$-$SiO_2$ trends in volcanoes of the Mariana arc, *Geology, 11*, 67-71, 1983.

Morrison, G. W., Characteristics and tectonic setting of the shoshinitic rock association, *Lithos, 13*, 97-108, 1980.

Reagan, M., and A. Meijer, Geology and geochemistry of early arc-volcanic rocks from Guam, *Geol. Soc. Am. Bull., 95*, 701-713, 1984.

Stern, R. J., On the origin of andesite in the Northern Mariana island arc: Implications from Agrigan, *Contrib. Mineral. Petrol., 68*, 207-219, 1979.

Stern, R. J., A common mantle source for western Pacific island arc and "hot-spot" magmas--implications for layering in the upper mantle, *Year Book Carnegie Inst. Washington., 80*, 455-461, 1981.

Stern, R. J., and L. Bibee, Esmeralda Bank: Geochemistry of an active submarine volcano in the Mariana Island arc, *Contrib. Mineral. Petrol., 86*, 159-169, 1984.

Stern, R. J., and E. Ito, Trace-element and isotopic constraints on the source of magmas in the active Volcano and Mariana island arcs, western Pacific, *J. Volcanol. Geotherm. Res., 18*, 461-482, 1983.

Stern, R. J., N. C. Smoot, and M. Rubin, Unzipping of the Volcano arc, Japan, *Tectonophysics, 102*, 153-174, 1984.

Stern, R. J., S. H. Bloomer, P. N. Lin, and N. C. Smoot, Submarine arc volcanism in the southern Mariana Arc as an ophiolite analog, *Tectonophysics, in press*, 1988a.

Stern, R. J., P. N. Lin, S. H. Bloomer, E.Ito, and J. Morris, LIL-and LREE-enriched magmatism in Mariana Arc Seamounts: Effect of propagating back-arc extension, *Geology, 16*, 426-430, 1988b .

Tarney, J., S. D. Weaver, A. D. Saunders, R. J. Pankhurst, and P. F. Barker, Volcanic evolution of the northern Antarctic Peninsula and the Scotia Arc in *Andesites: Orogenic Andesites and Related Rocks*, edited by R. S. Thorpe, pp. 371-400, John Wiley, New York, 1982.

Tsuya, H., Geology and petrography of Io-Sima (Sulphur Island), Volcano Islands Group, *Bull. Earthquake Res. Inst., 14*, 453-480, 1936.

Vogt, P. R., A. Lowrie, D. R. Bracey, and R. N. Hey, Subduction of aseismic ocean ridges: effects on shape, seismicity, and other characteristics of consuming plate boundaries, *Geol. Soc. Am. Spec. Pap. 172*, 59 pp., 1976.

Watson, E. B., and F. J. Ryerson, Rutile saturation in magma: implications for Nb-Ta-Ti depletion in orogenic magmas, *Eos Trans. AGU, 67*, 412, 1986.

Whitford, D. J., and I. A. Nicholls, Potassium variations in lava across the Sunda Arc, in *Volcanism in Australasia*, edited by R. W. Johnson, pp. 63-76, Elsevier, New York, 1976.

Wood, D. A., N. G. Marsh, J. Tarney, J. L. Joron, P. Fryer, and M. Treuil, Geochemistry of igneous rocks recovered from a transect across the Mariana Trough, Arc, Fore-arc, and Trench, sites 453

through 461, Deep Sea Drilling Project leg 60, *Initial Rep. Deep Sea Drill. Proj., 60*, 611-633, 1981.

Woodhead, J. D., and D. G. Fraser, Pb, Sr, and Be isotopic studies of volcanic rocks from the northern Mariana islands: implications for magma genesis and crustal recycling in the western Pacific, *Geochim. Cosmochim. Acta, 49*, 1925-1930, 1985.

Yoshida, T., S. Fujiwara, T. Ishii, and K. Aoki, Geochemistry of Fukutoku-Oka-noba submarine volcano, Izu-Ogasawara arc, *Res. Rep. Lab. Nucl. Sci. Tohoku Univ., 20*, 202-215, 1987.

Yuasa, M., Sofugan Tectonic Line, a new tectonic boundary separating northern and southern parts of the Ogasawara (Bonin) Arc, NW Pacific, in *Formation of Active Ocean Margins*, edited by N. Nasu, K. Kobayshi, S. Uyeda, I. Kushiro, and H. Kagami, pp. 483-496, Terra Scientific Publishing, Tokyo, 1985.

Yuasa, M., and K. Tamaki, Basalt from Minami-Iwo Jima Island, Volcano Islands, *Bull. Geol. Survey Jpn, 33*, 531-540, 1982.

S. H. Bloomer, Department of Geology, Boston University, Boston, MA 02215

E. Fisk and C. H. Geschwind, Department of Geology, Duke University, Box 6729, College Station, Durham, NC 27708

R. J. Stern, Center for Lithospheric Studies, University of Texas at Dallas, Richardson, TX 75083

(Received October 23, 1987;
revised June 20, 1988;
accepted August 23, 1988.)